



# CREaTE

Canterbury Research and Theses Environment

Canterbury Christ Church University's repository of research outputs

<http://create.canterbury.ac.uk>

Please cite this publication as follows:

Gomez-Paccard, M., Catanzariti, G., Ruiz-Martinez, VC, McIntosh, G., Nunez, J., Osete, M., Chauvin, A., Lanos, P., Bernal-Casasola, D. and Thiriot, J. (2006) A catalogue of Spanish archaeomagnetic data. *Geophysical Journal International*, 166 (3). pp. 1125-1143. ISSN 0956-540X.

Link to official URL (if available):

<http://dx.doi.org/10.1111/j.1365-246X.2006.03020.x>

This version is made available in accordance with publishers' policies. All material made available by CReaTE is protected by intellectual property law, including copyright law. Any use made of the contents should comply with the relevant law.

Contact: [create.library@canterbury.ac.uk](mailto:create.library@canterbury.ac.uk)



# A catalogue of Spanish archaeomagnetic data

M. Gómez-Paccard,<sup>1,2,3</sup> G. Catanzariti,<sup>2</sup> V. C. Ruiz-Martínez,<sup>2</sup> G. McIntosh,<sup>2</sup> J. I. Núñez,<sup>2</sup> M. L. Osete,<sup>2</sup> A. Chauvin,<sup>1</sup> Ph. Lanos,<sup>3</sup> D. H. Tarling,<sup>4</sup> D. Bernal-Casasola,<sup>5</sup> J. Thiriot<sup>6</sup> and ‘Archaeological Working Group’\*

<sup>1</sup>Géosciences-Rennes, CNRS, UMR 6118, University of Rennes 1, Campus de Beaulieu, 35042, Rennes, Cedex, France.

E-mail: miriam.gomez@univ-rennes1.fr

<sup>2</sup>Facultad de Ciencias Físicas, Universidad Complutense de Madrid, Ciudad Universitaria, 28040, Madrid, Spain

<sup>3</sup>Civilisations Atlantiques et Archéosciences, CNRS, UMR 6566, University of Rennes 1, Campus de Beaulieu, 35042, Rennes, Cedex, France

<sup>4</sup>Department Geological Sciences, University Plymouth, Drake Circus, Plymouth, PL4 8AA, UK

<sup>5</sup>Facultad de Filosofía y Letras, Universidad de Cádiz, 11003 Cádiz, Spain

<sup>6</sup>Laboratoire d’archéologie médiévale méditerranéenne, CNRS, UMR 6572, Maison méditerranéenne de Sciences de l’Homme, 13094, Aix-en-Provence, Cedex 2, France

Accepted 2006 March 20. Received 2006 March 19; in original form 2005 October 19

## SUMMARY

A total of 58 new archaeomagnetic directions has been determined from archaeological structures in Spain. Together with five previous results they allow the compilation of the first archaeomagnetic catalogue for Spain, which includes 63 directions with ages ranging between the 2nd century BC and the 20th century AD. Characteristic remanence directions have been obtained from stepwise thermal and alternating field demagnetization. The hierarchical structure has been respected in the calculation of the mean site directions. Rock magnetic experiments reveal that the main magnetic carrier is magnetite or titanomagnetite with different titanium contents. The age estimate of the studied structures is generally well justified by archaeological constraints. For six structures the proposed date is also supported by physical methods. The data are in close agreement with the French secular variation (SV) curve. This catalogue represents the first step in the construction of a SV curve for the Iberian Peninsula, which will be of much use in archaeomagnetic dating and in modelling of the Earth’s magnetic field in Western Europe.

**Key words:** archaeomagnetism, geomagnetic secular variation, Spain, Western Europe.

## 1 INTRODUCTION

In order to use archaeomagnetism as a dating tool a reliable reference curve has to be constructed for the region in question. For this purpose, the study of well-dated archaeological structures is required. Such structures include kilns, ovens, thermal baths and burnt walls, or any heated material that has recorded the Earth’s magnetic field during its cooling and thus acquired a thermoremanent magnetization (TRM) parallel to the ambient field. The reference curves—called secular variation (SV) curves—can be used as a dating tool by comparing the archaeomagnetic field information (direction and/or intensity) of archaeological material with the known SV curve of the Earth’s magnetic field for this area. More or less well-defined SV curves covering the last millennia are available for different countries in Europe (Kovacheva & Toshkov 1994; Batt 1997; Gallet

*et al.* 2002; Schnepf & Lanos 2005) and this dating method is currently in use. The large number of excavations carried out in the past or that are now in progress in Spain means that the potential of this technique in the Iberian Peninsula is great. However, despite such potential there is a lack of archaeomagnetic data available for the region, a deficit addressed here.

This study consists of a compilation of previously available results for Spain, along with the results of the study of 58 new structures, giving rise to a catalogue of 63 archaeomagnetic directions. The principal information related to each individual study has been detailed, including the field sampling and laboratory treatment, and the criteria used in the determination of the characteristic directions, at the specimen, sample and site level. Rock magnetic studies have been carried out to identify the main magnetic minerals carrying the archaeomagnetic signal. The archaeological and chronological information has also been compiled and analysed, and is presented as an appendix.

This work is the first example of an intensive cooperation between archaeologists and geophysicists in Spain in the field of archaeomagnetism and establishes the basis of future archaeomagnetic research. The catalogue presented represents the first step in the construction

\*A, Sáez-Espigares, I. García-Villanueva, J.A. Gisbert-Santonja, M.A. Hervás, P. Jiménez-Castillo, M. Mesquida-García, I. Navarro, M. Orfila-Pons, I. Ramírez-González, M. Retuerce, D. Urbina and C. Urquijo.

of a reliable SV curve for the Iberian Peninsula. The data set further contributes to better constraining the variation of the Earth's magnetic field in Western Europe during the two last millennia.

## 2 PREVIOUS ARCHAEOMAGNETIC STUDIES IN SPAIN

The first published result from Spain was from Ampurias, Cataluña (Thellier 1981). The pioneer of archaeomagnetism studied one Spanish kiln dated between 200 BC and 100 AD and provided the first archaeomagnetic direction for this region. The next results were from La Maja, in La Rioja, and Villa del Pañuelo, in Madrid. At La Maja, Parés *et al.* (1992) studied a Roman pottery kiln, whose abandonment was dated by archaeological constraints as being in the 1st century AD. They confirmed the previous archaeological date by referring the obtained inclination to the French SV curve, giving an age of 30–78 AD. The archaeological date (1st century AD) has been retained in this catalogue. Kovacheva *et al.* (1995) conducted an archaeointensity study using the same sample collection and confirm, by comparison with archaeointensity data from neighbouring countries, the date estimated by Parés *et al.* (1992). Two Roman kilns were studied at Villa del Pañuelo, Madrid (Oyamburu *et al.* 1996), which were also dated using the French SV curve, giving ages of 0–150 AD and 150–350 AD. The results obtained are consistent with later archaeological dating. The archaeological date has been retained in this catalogue. There are unpublished results available from the Roman ovens of Arva and Celti (in Seville), studied by Evans (private communication, 1985). Although not well dated at the time of their study, the archaeomagnetic results demonstrated that these ovens were not coeval and that a difference of approximately 50–100 yr existed between their use. Recent archaeological studies now place the Arva oven between 150 and 250 AD (Remesal, private communication, 2002). These five directions have been included in the catalogue. Nachasova *et al.* (2002) published an archaeointensity study of ceramic fragments from Valencia dated

between the 5th and 2nd centuries BC. These data, concerning only archaeointensity determinations, are not included in the catalogue but can be found in Korte *et al.* (2005).

## 3 NEW ARCHAEOMAGNETIC STUDIES

### 3.1 Sampling

The locations of the new structures that have been investigated are shown in Fig. 1. Most of the structures are kilns, but one furnace, two thermal baths, two burnt walls and a burnt floor have also been studied. The types of material sampled include burnt clay, bricks and native rock, depending on the construction of the particular structures. Three types of independently oriented samples were taken in the field. For well-consolidated structures oriented core samples were taken using portable rock drills of the type commonly used in palaeomagnetic studies (drill samples in Table 1). Alternatively, especially for less well-consolidated structures, large block samples were taken by preparing a flat surface using gypsum plaster, which was then oriented (block samples in Table 1). In the case of poorly consolidated material the samples were completely encased in plaster before removal. Smaller hand samples were occasionally taken using the method described by Tarling (1983). Here small, wooden cylinders were fixed to the material to be sampled. These were oriented and removed, with a small amount of material staying fixed to the cylinders (hand samples in Table 1). Orientation in the vertical plane was achieved using a compass and/or inclinometer, and in the horizontal plane using spirit levels, magnetic and solar compasses. At least four, but generally more than eight, independently oriented samples were taken from each archaeological structure ( $N'$  in Table 1).

In the laboratory, standard cylindrical specimens (volume = 10.8 cm<sup>3</sup>) were prepared from the cored and block samples. Poorly consolidated samples from five sites were treated using sodium silicate ('waterglass') or ethyl silicate ('Silbond 40',) prior to taking

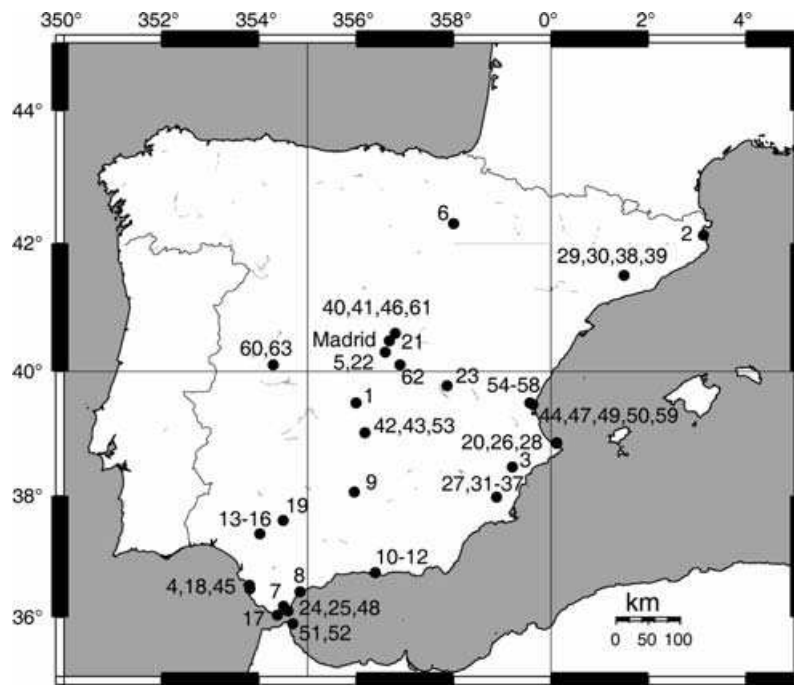


**Figure 1.** Map showing the location of archaeomagnetic sites included in the catalogue. Madrid (40.4°N, 3.7°W) has been chosen as the reference site for Spain.

**Table 1.** Archaeomagnetic directions from Spanish sites.

No	Name	$t_{\min}$	$t_{\max}$	$t_{\text{mean}}$	Meth.	$N/(n/n)/N$	$D_s$	$I_s$	$D_m$	$I_m$	$k$	$\alpha_{95}$	Site	Structure	Samples	Lat (°N)	Long (°E)	Treat.	ChRM	RM	Lab.	Reference
1	PLM	-150	-50	-100	arch/C14	8/(9/9)/8	-4.0	58.2	-4.1	59.0	182	4.1	Plaza de Moros	pottery kiln	drill	39.50	-4.00	AF/Th	PCA		M	
2	AMP	-200	100	-50	arch	4	-8.5	63.5	-7.7	62.7	2592	1.5	Ampurias	kiln	block	42.12	3.13	NRM	PCA			Thellier (1981)
3	MON	-50	35	-7.5	arch	21/(12/9)/9	0.3	57.3	0.3	59.1	546	2.2	El Monastil	pottery kiln	drill	38.47	-0.79	AF	PCA		M	
4	GA	40	50	45	arch	11/(10/7)/7	3.8	53.4	4.1	57.4	150	4.9	El Gallinero	pottery kiln	hand	36.53	-6.19	AF/Th	PCA		P	
5	VIL1	0	100	50	arch	25	-5.5	57.1	-5.5	57.2	116	2.6	Villa del Pañuelo I	kiln	drill	40.30	-3.40	Th	PCA		M	Oyamburu <i>et al.</i> (1996)
6	LMA	0	100	50	arch	29	-0.8	58.4	-0.9	56.6	128	2.1	Calahorra, La Maja	pottery kiln	drill	42.27	-2.02	AF/Th	PCA			Parés <i>et al.</i> , 1992
7	COS	0	100	50	arch	14/(23/14)/14	3.7	54.3	4.0	58.2	46	6.0	Costalita	kiln	drill	36.42	-5.15	AF/Th	PCA		M	
8	VC	80	90	85	arch	31/(34/27)/27	2.1	46.7	2.5	51.6	146	2.3	Venta del Carmen	pottery kiln	hand/ drill	36.18	-5.49	AF/Th	PCA		P/M	
9	VIA	50	150	100	arch	10/(10/9)/9	1.4	50.5	1.5	53.0	259	3.2	Villares Andujar	pottery kiln	drill	38.06	-4.04	AF	PCA		M	
10	CAR-HI	50	150	100	arch	7/(8/8)/7	-1.7	55.3	-1.8	58.4	293	3.5	Cartuja I	pottery kiln	drill	37.18	-3.10	AF/Th	PCA		M	
11	CAR-HII	50	150	100	arch	9/(11/9)/7	-3.1	52.2	-3.3	55.5	125	5.4	Cartuja II	pottery kiln	drill	37.18	-3.10	AF/Th	PCA		M	
12	CAR-HIII	50	150	100	arch	5/(8/7)/5	2.9	52.3	3.0	55.6	392	3.9	Cartuja III	pottery kiln	drill	37.18	-3.10	AF/Th	PCA		M	
13	PAR1	90	130	110	arch	14/(10/10)/10	-2.4	53.0	-2.3	56.1	484	2.2	Patio Cardenal I	pottery kiln	drill	37.38	-5.98	AF	PCA		M	
14	PAR3	90	130	110	arch	13/(6/6)/6	-4.1	54.1	-4.1	56.9	324	3.7	Patio Cardenal III	pottery kiln	drill	37.38	-5.98	AF	PCA		M	
15	PAR4	90	130	110	arch	13/(8/7)/7	-2.7	53.3	-2.4	56.3	1026	1.9	Patio Cardenal IV	pottery kiln	drill	37.38	-5.98	AF	PCA		M	
16	PAR5	90	130	110	arch	20/(17/17)/17	-4.3	53.5	-4.3	56.4	193	2.6	Patio Cardenal V	pottery kiln	drill	37.38	-5.98	AF	PCA		M	
17	BC	100	150	125	arch	16/(16/14)/14	-2.2	46.7	-2.0	51.6	145	3.6	Baello Claudia	baths	drill	36.03	-5.62	AF	RC+PCA(6)		M	
18	GAL	100	220	160	arch	11/(12/8)/7	-0.1	55.8	-0.1	59.4	176	4.6	Gallineras	pottery kiln	drill	36.47	-6.18	AF/Th	PCA		M	
19	ARV	150	250	200	arch	17	-3.7	51.8	-3.6	54.6	682	1.3	Arva	kiln		37.60	-5.50					Evans, personal communication
20	DENA	220	250	235	arch	13/(10/10)/10	-4.5	52.6	-5.0	54.5	669	1.9	Setla Mirarosa Miraflor	kiln	block	38.86	0.02	TH	PCA	AT, C	R	
21	HIP	225	325	275	arch	22/(23/18)/18	-4.0	52.6	-4.1	52.5	104	3.4	Hyppolytus	baths	drill	40.48	-3.32	AF/Th	PCA		M	
22	VIL2	250	350	300	arch	31	-2.7	51.7	-2.6	51.7	131	2.2	Villa del Pañuelo II	kiln	drill	40.30	-3.40	Th	PCA		M	Oyamburu <i>et al.</i> , 1996
23	VAL	270	330	300	arch	18/(24/7)/7	-5.4	48.0	-5.8	48.9	58	9.7	Valeria	burnt wall	drill	39.77	-2.13	AF/Th	RC		M	
24	PG1	400	410	405	arch	14/(14/13)/13	-14.1	46.4	-14.3	50.8	33	7.3	Puente Grande I	pottery kiln	drill	36.18	-5.49	AF	PCA		M	
25	PG2	400	410	405	arch	23/(18/15)/15	0.3	52.5	0.4	56.7	129	3.4	Puente Grande II	pottery kiln	drill	36.18	-5.49	AF	PCA		M	
26	RO2	1000	1050	1025	arch	15/(18/14)/14	17.3	50.9	16.8	51.6	100	4.0	Ramon Ortega II	pottery kiln	hand	38.86	0.12	AF	PCA		P	
27	MURG	1000	1100	1050	arch	21/(8/8)/8	21.7	51.3	21.8	52.9	1437	1.5	Murcia c/Sagasta	glass making kiln	block	37.98	-1.12	TH	PCA	AT, C	R	
28	RO1	1050	1100	1075	arch	20/(20/16)/16	15.8	47.9	15.2	48.7	380	1.9	Ramon Ortega I	pottery kiln	hand	38.86	0.12	AF	PCA		P	
29	CDAP	1010	1220	1115	C14	11/(17/8)/8	3.6	50.6	2.5	49.1	236	3.6	Cabrera d'Anoia	pottery kiln	block	41.50	1.50	AF/TH	PCA	C	R	
30	CDAU	1029	1203	1116	C14	14/(12/6)/6	9.6	45.7	8.0	43.6	2765	1.3	Cabrera d'Anoia	pottery kiln	block	41.50	1.50	AF/TH	PCA	C	R	

Table 1. (Continued.)

No.	Name	$t_{\min}$	$t_{\max}$	$t_{\text{mean}}$	Meth.	$N'/(n'/n)/N$	$D_s$	$I_s$	$D_m$	$I_m$	$k$	$\alpha_{95}$	Site	Structure	Samples	Lat (°N)	Long (°E)	Treat.	ChRM	RM	Lab.	Reference
31	MURO	1100	1200	1150	arch/his	6/(7/6)/6	13.6	44.7	13.2	47.1	308	3.8	Murcia c/Puxmarina	kiln	block	37.98	-1.12	TH	PCA	AT, C	R	
32	MURN	1100	1200	1150	arch/his	19/(7/6)/6	14.0	45.1	13.7	47.3	1038	2.1	Murcia c/Puxmarina	kiln	block	37.98	-1.12	TH	PCA	AT, C	R	
33	MURM	1100	1200	1150	arch/his	15/(10/7)/7	14.9	45.5	14.6	47.7	811	2.1	Murcia c/Puxmarina	kiln	block	37.98	-1.12	TH	PCA	AT, C	R	
34	MURL	1100	1200	1150	arch/his	16/(9/9)/9	16.2	44.2	15.8	46.4	1842	1.2	Murcia c/Puxmarina	kiln	block	37.98	-1.12	TH	PCA	AT, C	R	
35	MURI	1100	1200	1150	arch/his	15/(13/7)/7	15.2	41.7	14.8	44.0	215	4.1	Murcia c/Puxmarina	kiln	block	37.98	-1.12	TH	PCA	AT, C	R	
36	MURK	1100	1200	1150	arch/his	16/(13/9)/9	14.1	45.2	13.8	47.4	547	2.2	Murcia c/Puxmarina	kiln	block	37.98	-1.12	TH	PCA	AT, C	R	
37	MURH	1100	1200	1150	arch/his	15/(20/10)/10	17.3	46.4	17.1	48.4	330	2.7	Murcia c/Puxmarina	kiln	block	37.98	-1.12	TH	PCA	AT, C	R	
38	CDAJ	1056	1262	1159	C14	12/(11/8)/8	9.0	45.2	7.4	43.1	416	2.7	Cabrera d'Anoia	pottery kiln	block	41.50	1.50	AF/TH	PCA	C	R	
39	CDAH	1043	1281	1162	C14	10/(11/5)/5	10.7	46.4	9.1	44.3	3461	1.3	Cabrera d'Anoia	pottery kiln	block	41.50	1.50	AF/TH	PCA	C	R	
40	MAGI	1250	1300	1275	arch	14/(14/5)/5	11.5	42.6	11.3	42.2	500	4.8	Magisterio I	pottery kiln	drill	40.63	-3.16	Th	RC		M	
41	MAGII	1250	1300	1275	arch	16/(16/6)/6	4.1	47.3	4.0	47	179	6.1	Magisterio II	pottery kiln	drill	40.63	-3.16	Th	RC+PCA(1)		M	
42	CALA	1275	1300	1287.5	arch/his	16/(9/8)/8	11.4	44.9	11.6	46.5	356	2.9	Calatrava la Vieja	pottery kiln	block	39.02	-3.82	TH	PCA	AT, C	R	
43	CALB	1275	1300	1287.5	arch/his	14/(12/10)/10	7.1	44.4	7.2	46.2	284	2.9	Calatrava la Vieja	pottery kiln	block	39.02	-3.82	TH	PCA	AT, C	R	
44	VALN	1238	1350	1294	arch	20/(12/9)/9	2.1	46.6	1.3	47.7	1859	1.2	Valencia Velluters	bricks making kiln	block	39.47	-0.37	TH	PCA	AT, C	R	
45	CSR			1300	arch	10/(11/3)/3	8.1	46.0	8.9	51.0	298	7.2	Castillo de San Romualdo	kiln	drill	36.3	-6.1	AF/TH	PCA	H	M	
46	GUA1	1275	1325	1300	arch	4/(16/16)/4	14.3	57.8	14.2	57.5	1104	2.8	SUE-10	pottery kiln	hand	40.60	-3.20	AF/Th	PCA	H	M	
47	VALI	1238	1400	1319	arch	21/(13/11)/11	4.4	46.4	3.6	47.3	725	1.7	Valencia Velluters	bricks making kiln	block	39.47	-0.37	TH	PCA	AT, C	R	
48	BI	1369	1369	1369	hist	28/(30/12)/10	0.4	41.9	0.8	47.3	206	3.4	Av. Blas de Infante	burnt wall	drill	36.13	-5.45	AF/Th	PCA		M	
49	VALK	1300	1450	1375	arch	15/(9/9)/9	3.0	44.2	2.2	45.2	1606	1.3	Valencia Velluters	glass making kiln	block	39.47	-0.37	TH	PCA	AT, C	R	
50	VALM	1300	1450	1375	arch	16/(9/9)/9	7.2	47.0	6.5	47.8	2733	1.0	Valencia Velluters	glass making kiln	block	39.47	-0.37	TH	PCA	AT, C	R	
51	LLD	1400	1415	1407.5	arch/his	14/(15/15)/14	9.6	37.0	10.4	43.4	98	4.0	Llano las Damas	pottery kiln	hand	35.89	-5.30	AF/Th	PCA		M	
52	HR	1400	1415	1407.5	arch/his	8/(8/7)/7	7.8	35.9	8.6	42.4	417	3.1	Huerta Rufino	pottery kiln	drill	35.89	-5.30	AF/Th	RC+PCA(5)		M	
53	CALC	1400	1420	1410	arch/his	18/(9/8)/8	3.0	47.0	3.1	48.6	790	2.0	Calatrava la Vieja	pottery kiln	block	39.02	-3.82	TH	PCA	AT, C	R	
54	PATA	1450	1500	1475	arch	15/(18/10)/10	3.6	56.4	3.5	57.1	792	1.7	Paterna c/Huertos	pottery kiln	block	39.50	-0.43	TH	PCA	AT, C	R	
55	TMO	1490	1540	1515	arch	18/(18/16)/16	7.5	55.7	7.4	56.2	343	2.0	Paterna Testar del Moli	pottery kiln	drill	39.50	-0.43	AF	PCA		M	
56	PATJ	1429	1611	1520	C14	22/(17/16)/16	6.6	62.2	6.9	62.7	1201	1.1	Paterna Testar del Moli	pottery kiln	block	39.50	-0.43	TH	PCA	AT, C	R	
57	PATH	1450	1600	1525	arch	12/(15/10)/10	7.3	53.5	7.0	54.1	831	1.7	Paterna Testar del Moli	pottery kiln	block	39.50	-0.43	TH	PCA	AT, C	R	
58	PATB	1525	1650	1587.5	arch	20/(13/11)/11	5.8	64.1	6.4	64.6	827	1.6	Paterna c/Huertos	pottery kiln	block	39.50	-0.43	TH	PCA	AT, C	R	
59	VALL	1575	1625	1600	arch	19/(13/11)/11	9.1	56.6	9.0	57.1	557	1.9	Valencia Velluters	kiln	block	39.47	-0.37	TH	PCA	AT, C	R	
60	YUS1	1784	1814	1799	arch/his	8/(22/17)/7	-14.3	55.5	-14.3	55.5	173	4.6	Monastery at Yuste	kiln	hand/drill	40.10	-5.70	Th	PCA		M	
61	GUA2	1825	1845	1835	arch/his	13/(16/16)/13	-21.1	61.5	-21.1	61.4	238	2.7	Huertas del Carmen	furnace	drill	40.60	-3.20	AF	PCA	H	M	
62	AL	1830	1910	1870	arch/his	7/(20/11)/6	-14.2	63.0	-14.3	63.3	159	5.3	Palacio de Perales	burnt floor	hand	40.10	-3.10	Th	PCA	H	M	
63	YUS2	1959	1959	1959	his	5/(19/15)/5	-11.1	58.2	-11.0	58.2	138	6.5	Monastery at Yuste	kiln	hand	40.10	-5.70	Th	PCA	C	M	

Columns from left to right:

No., structure number; Name, name of the structure;  $t_{\min}$ , minimum age of the structure in years AD;  $t_{\max}$ , maximum age of the structure in years AD;  $t_{\text{mean}}$ , mean age of the structure in years AD; Meth., method of dating (arch.: archaeological age estimate, hist: historical document, C14: conventional  $^{14}\text{C}$ );  $N'/(n'/n)/N$ : number of independently oriented samples taken from the site ( $N'$ )/specimens analysed ( $N'$ )/taken into account in the calculation of the mean sample directions( $n$ )/samples taken into account in the calculation of the mean site direction ( $N$ );  $D_s$  and  $I_s$ , declination and inclination *in situ*;  $D_m$  and  $I_m$ , declination and inclination at the latitude of Madrid (40.4, -3.7);  $k$  and  $\alpha_{95}$ , precision parameter and 95 per cent confidence limit of characteristic remanent magnetization; Site, site name; Structure, kind of structure; Samples, type of samples (drill: drilled samples, hand: hand samples, block: large block samples); Lat and Long, site latitude and longitude; Treat., laboratory treatment (AF: alternating field demagnetization, Th: Thermal demagnetization, TH: Thermal demagnetization from Thellier palaeointensity experiments); ChRM, ChRM determination method (RC: remagnetization circles, PCA: principal component analysis—with number of PCA analyses when mixed with RC given in brackets); RM, rock magnetic experiments (AT: anisotropy of TRM, C: Curie temperature determination, H: hysteresis and IRM measurements); Lab., laboratory where measurements were made (M: Madrid, R: Rennes, P: Plymouth); Reference, blank space indicates this study.



the specimens. Several treatment techniques were used. The first involved cutting slices from the sample (from sites CDAJ, CDAH, CDAU and CDAP in Table 1), followed by a two-step impregnation using first 50–50 per cent then 20–80 per cent water-sodium silicate solution, both under vacuum.  $2 \times 2 \times 2$  cm<sup>3</sup> cubic specimens were then cut from the dried sample slice. Alternatively, the samples (from site GUA1 in Table 1) were immersed in ethyl silicate over a period of days, then taken out and dried (at room temperature). Standard cylindrical specimens were then drilled from the sample. Previous studies carried out in baked clays show that the impregnation with water glass does not significantly affect the remanence during heating experiments (Kostadinova *et al.* 2004).

### 3.2 Magnetic measurements

Measurements were performed in the palaeomagnetic and archaeomagnetic laboratories of the University Complutense de Madrid (Spain), Géosciences Rennes (France) and the University of Plymouth (UK). Remanent magnetization was measured using Molspin, JR5 (Agico) or Digico large sample spinner magnetometers. Stepwise alternating field (AF) demagnetization was carried out using Schonstedt or Molspin large demagnetizers, with five or more steps up to the maximum available field (100 or 150 mT). Stepwise thermal (Th) demagnetization was conducted using MMTD or Schonstedt ovens with five or more steps until more than 80 per cent of natural remanent magnetization (NRM) had been removed, unless thermally induced alteration took place, at which point demagnetization was halted. For the structures analysed at Rennes, the classical Thellier palaeointensity method (Thellier & Thellier 1959), with pTRM checks, based on the comparison between NRM lost and partial thermoremanent magnetization (pTRM) gained in a known laboratory field was used. The thermal demagnetization data were obtained from these experiments, denoted as TH in Table 1.

Low field magnetic susceptibility ( $K$ ) was measured for all specimens using Bartington or Kappabridge (KLY3, Agico) susceptibility meters.  $K$  was also measured after each heating step during Th and TH demagnetization in order to monitor mineralogical alteration. Thermomagnetic curves were measured in air using a KLY3 susceptibility meter with fitted furnace. Magnetic hysteresis was measured using a coercivity meter (Jasonov *et al.* 1998) with a maximum applied field of 500 mT. This instrument also generated stepwise acquisition and reverse-field acquisition of isothermal remanence (IRM).

TRM anisotropy has been determined for all specimens from 21 of the 25 structures measured in Rennes (AT in Table 1). To achieve this, TRM acquisition in six directions was carried out after demagnetizing the NRM to 70 per cent of its initial value, followed by a thermal stability check along the specimen cylindrical axis. The NRM and TRM measurements were corrected for anisotropy using the method described by Veitch *et al.* (1984) and Chauvin *et al.* (2000). All specimens used to calculate mean directions of magnetization from these 21 structures have been corrected for TRM anisotropy.

## 4 NEW RESULTS

### 4.1 Archaeological dating

In order to propose an interval of age for each structure a critical analysis of the compiled archaeological information was carried out.

The *terminus post-quem* (TPQ) and the *terminus ante-quem* (TAQ), proposed by archaeologists or by radiocarbon studies, are given where available. The TPQ (TAQ) refers to the date after (before) which the structure may have been in use. The TPQ, generally easier to determine than the TAQ, is commonly determined on the basis of the age of the oldest objects found in the same stratigraphic unit as the analysed structure. The TAQ is generally established on the basis of the abandonment of the site, ceramics and/or burial/infilling of the abandoned structure. These two parameters are the principal support of the proposed ages. A description of each archaeological site and structure is given in the Appendix, together with some references that may be useful for future archaeomagnetic studies. The ages ascribed to each of the structures included in the catalogue are shown in Table 1.

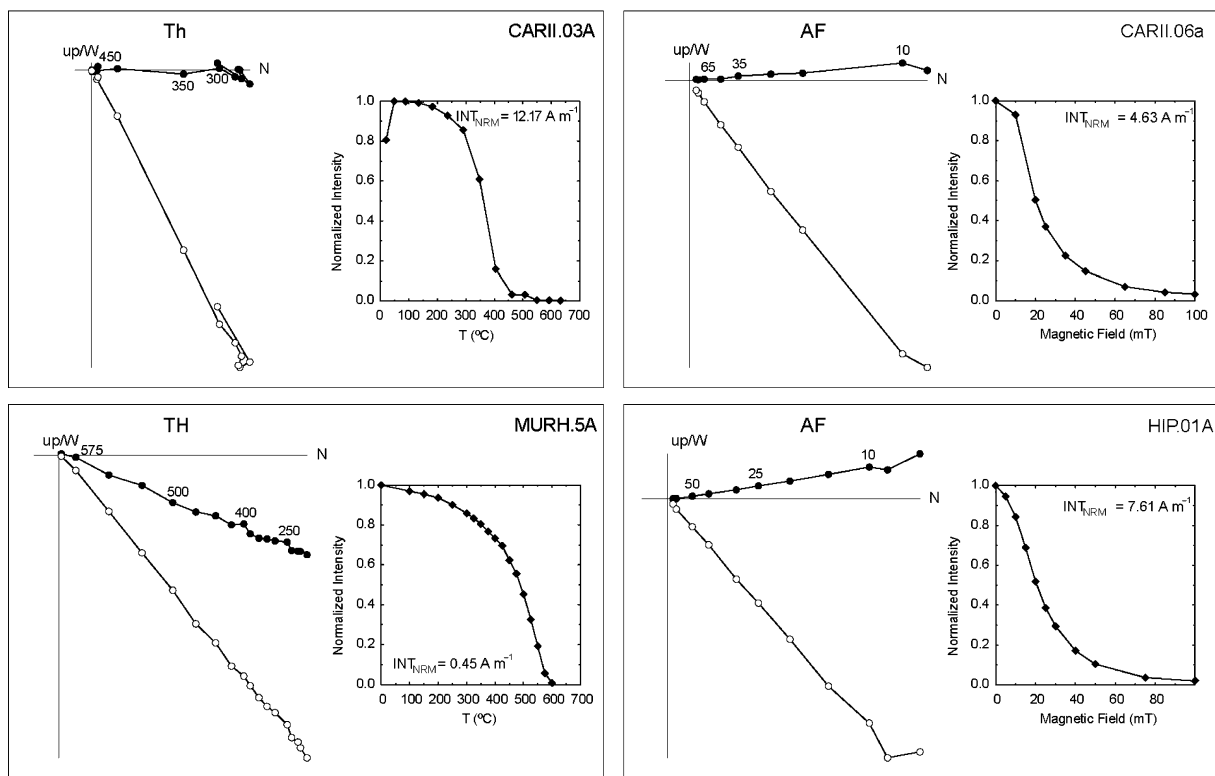
Six of the analysed structures have been dated by the radiocarbon method. At the Plaza de Moros site (1, PLM, in Table 1), conflictive radiocarbon dates were obtained from samples from the same burnt wooden beam used in the dating experiment. The younger of the dates (200 BC–20 AD) is consistent with the archaeologically determined date (150–50 BC). The archaeological date has been retained in the catalogue. At the Avenida Blas de Infante site (48, BI, in Table 1) the year of the fire associated with the sampled structure is precisely controlled by historical documents, whereas at the Yuste site (63, YUS2, in Table 1) anecdotal evidence describes a modern kiln used in 1959 AD. A further 15 structures include some form of historical constraints on the definition of their TPQ/TAQ. The remaining structures are dated on the basis of archaeological information. Great care has been taken in collecting and assessing this information and the basis of the archaeological constraints for each site and structure is set out in the Appendix. In future studies it would be of great interest to constrain archaeological information by other physical dating techniques, and to describe the stratigraphic constraints between the studied structures. Lanos (2004) demonstrates that such information may be taken into account in the construction of SV curves.

### 4.2 Demagnetization of NRM

NRM demagnetization results were visually inspected using orthogonal and stereographic projections. In many cases a variable, unstable component was removed at low temperatures or fields (<200°C or <2–10 mT). This is interpreted as a viscous overprint and is not considered further. Specimens from all but five structures exhibited a single stable component. Well-defined, linear trajectories trending to the origin of the orthogonal projection were isolated by both Th/TH and AF demagnetization and remanence directions were calculated using principal component analysis (Kirschvink 1980). Two types of behaviour could be distinguished within this group of specimens on the basis of the NRM intensity decay curves.

The first type of behaviour, called group 1A in Fig. 2, includes specimens exhibiting a single unblocking temperature ( $T_{ub}$ ) or coercivity spectrum. AF demagnetization produced monotonic NRM intensity decay curves and more than 90 per cent of NRM was demagnetized by 100 mT (CARI.06A, HIP.01A, Fig. 2). Thermal demagnetization revealed monotonic intensity decays, with a range of maximum  $T_{ub}$ s of between 300°C and 625°C. In most cases a maximum  $T_{ub}$  of between 500°C and 600°C was observed (e.g. MURH.5A, Fig. 2).  $T_{ub}$ s of 290–320°C were also common, as were  $T_{ub}$ s of around 400–450°C (e.g. CARI.03A, Fig. 2). In all of these cases there is no evidence of a further, higher-temperature component and the NRM vector passes through the origin of the orthogonal vector plots.

## Group 1A



## Group 1B

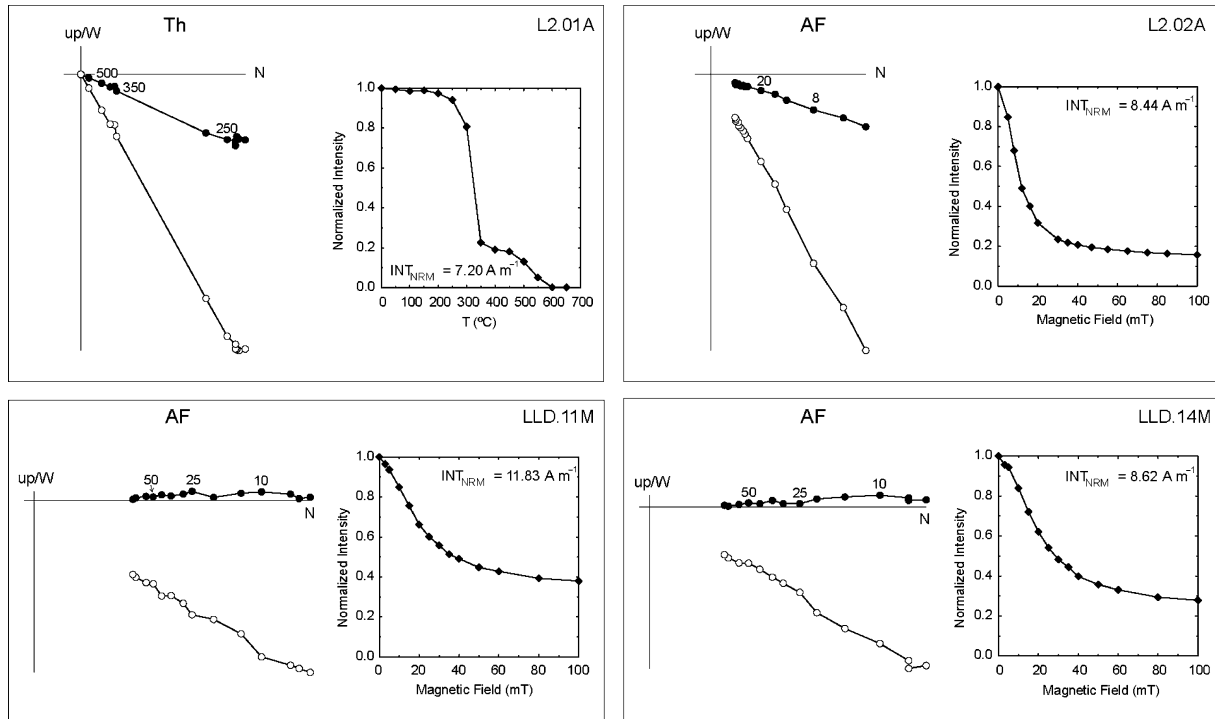


**Figure 2.** Representative plots for Type 1 and Type 2 NRM demagnetization behaviour (see text for explanation). Orthogonal vector plots [solid (open) symbols: projection upon horizontal (vertical) plane] and normalized intensity decay plots are shown on the left- and right-hand side, respectively. TH/Th/AF refer to thermal demagnetization from Thellier-type palaeointensity experiments/thermal demagnetization/alternating field demagnetization, respectively.

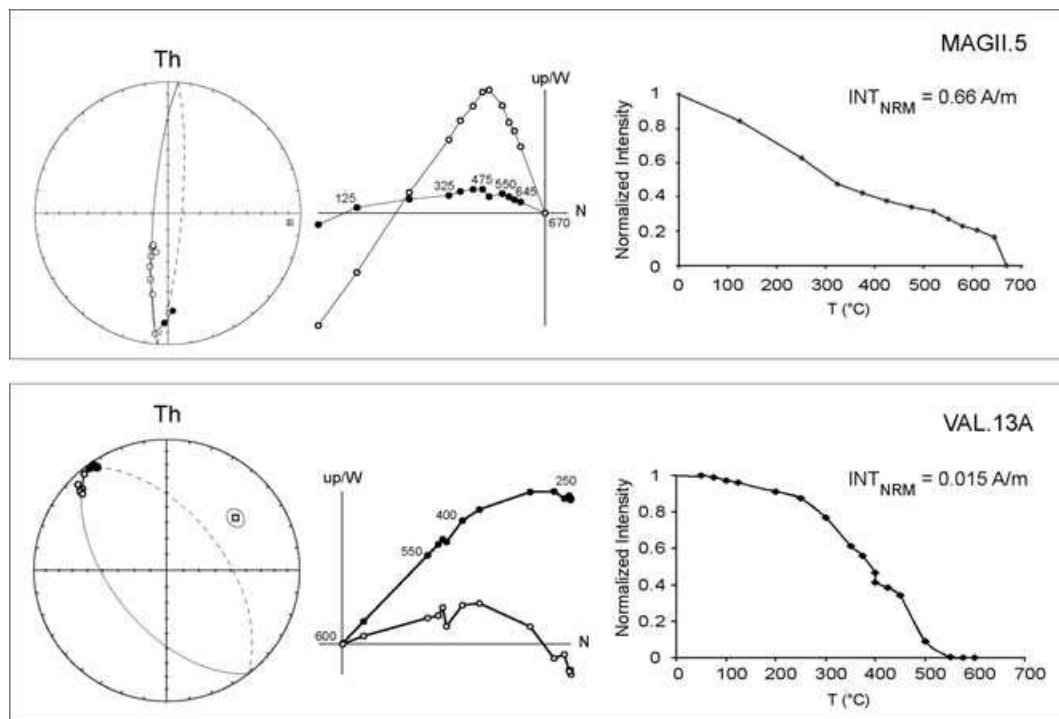


**Figure 3.** Representative plots for complex NRM demagnetization behaviour (see text for explanation). Stereographic projections (solid symbols: projection on the lower hemisphere), orthogonal vector plots and normalized intensity decay plots are shown from left to right. The great circles used to calculate directions are shown on the stereographic projections.

The second type of behaviour (called group 1B in Fig. 2) includes specimens with two  $T_{ub}$ /coercivity spectra. Here there are two magnetic phases carrying the single, stable component. AF demagnetization lead to NRM decreases up to 100 mT, but with more than 20 per cent remaining undemagnetized (e.g. L2.02A, LLD.11M, LLD.14M, Fig. 2). This type of specimen is considered as having a low-coercivity phase and an (undefined) high-coercivity phase. Th/TH demagnetization defined two spectra at different temperatures. Different spectra were recognized on the basis of clear slope changes on the intensity decay plot (e.g. L2.01A, Fig. 2).

Five structures exhibited complex NRM demagnetization behaviour, with two stable components of magnetization (MAGII.5, VAL.13A, Fig. 3). Th/TH demagnetization was generally better than AF at isolating the two components. Where linear segments of both components could be isolated on the orthogonal projection, remanence directions were calculated as previously described. This was not generally possible, as in most cases there was considerable overlap of the  $T_{ub}$ /coercivity spectra associated with the two directions. Here the low-temperature or low-coercivity phase was defined by great-circle analysis of the stereographic projection of the NRM vector (Fig. 3), calculating a pole direction defining the best-fit plane of the great circle traced by the vector endpoint after each demagnetization step.

### 4.3 Rock magnetic properties

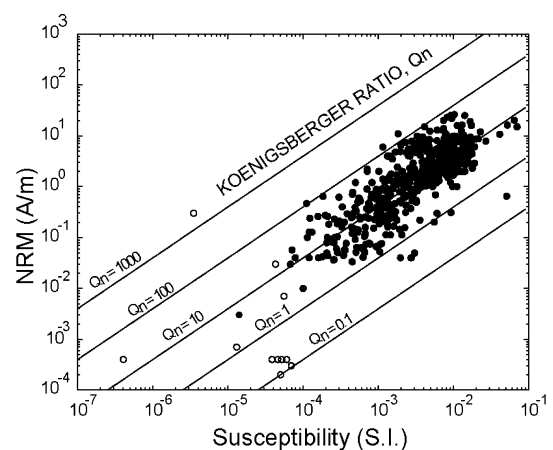
#### 4.3.1 NRM-K

Fig. 4 shows the intensity of the NRM (A/m) plotted versus  $K$  (SI), indicating Koenigsberger ratio ( $Q_n$ ) isolines. The specimens have been divided into two groups: specimens from structures heated to low temperatures (e.g. burnt walls/floors, VAL, BI and ALG in

Table 1, open circles in Fig. 4) and specimens from well-heated structures (all remaining structures, solid circles in Fig. 4). Both NRM and  $K$  vary by several orders of magnitude, giving values of  $Q_n$  generally between 1 and 100. This high variability is due to the different materials used in the construction of the structures. The specimens corresponding to the less heated materials generally present lower NRM and  $K$  values.

#### 4.3.2 Thermomagnetic curves

The variation of bulk susceptibility with temperature ( $KT$  curve) was determined for more than 140 samples from 26 structures (C



**Figure 4.** NRM intensity (A/m) versus bulk susceptibility (SI) for specimens from partially heated (white circles, structures 23, 50 and 62 in Table 1) and well-heated (black circles) structures. Koenigsberger ratio isolines are shown.



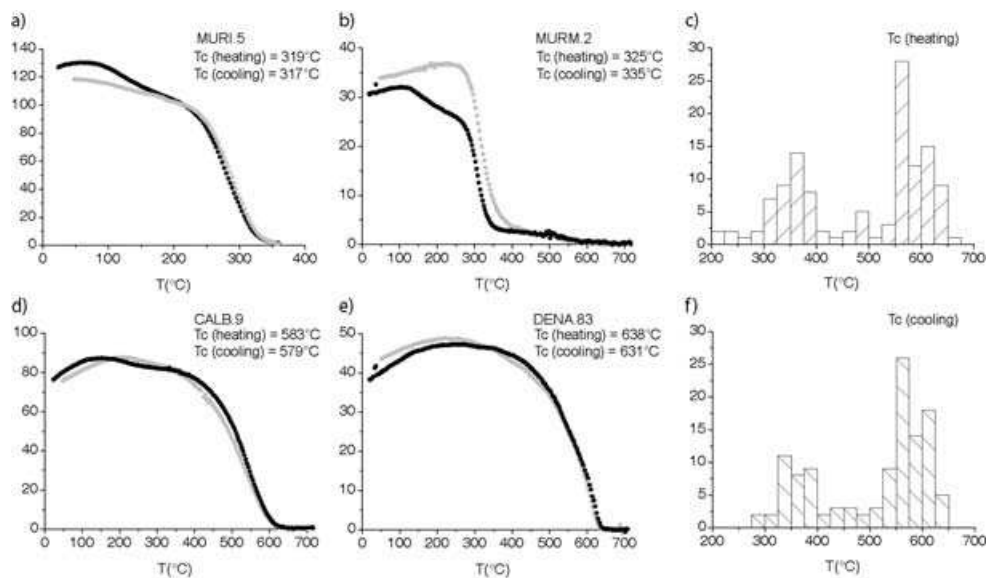


**Figure 5.** Representative thermomagnetic curves. Susceptibility is plotted on the  $y$ -axis in arbitrary units. Heating/cooling are shown in black/grey. The distributions of Curie temperatures ( $T_c$ ), calculated from the heating (c) and cooling (f) branches of the curves, are shown.

in Table 1), from which the Curie temperatures ( $T_c$ ) have been calculated using the first and second derivative method described by Tauxe (1998). In some cases smoothing of the data was needed due to the low  $K$  values and subsequent bad signal to noise ratio. Occasionally  $T_c$  could not be determined because of the low  $K$  values. Representative thermomagnetic curves are given in Fig. 5, along with a histogram of  $T_c$ s obtained.

The majority of the  $KT$  curves are relatively reversible, showing that the magnetic carriers are thermally stable. An unstable magnetic phase is sometimes observed around 200°C on the heating curve, which is absent on the cooling curve (e.g. MURI.5, Fig. 5). This may point to the presence of goethite. The  $T_c$ s obtained are in agreement with the unblocking temperatures found in the thermal demagnetization of NRM. Four types of behaviour, but two principal types, were found. In most cases  $T_c$ s of between 540°C and 585°C were observed (e.g. CALB.9, Fig. 5), suggesting that the principal magnetic carrier is magnetite or Ti-poor titanomagnetite. The other main group of samples exhibited  $T_c$ s of between 270 and 420°C (e.g. MURI.5, Fig. 5), and these phases dominate even if a high  $T_c$  phase is also present (e.g. MURM.2, Fig. 5). Similar low Curie temperatures have been also observed by other authors (Casas *et al.* 2005; Schnepf *et al.* 2004; Chauvin *et al.* 2000) in bricks and baked clays. Another less important group of samples gives  $T_c$ s between 435°C and 510°C, suggesting that in this case the magnetic carrier is titanomagnetite with higher Ti content. The last group of samples shows  $T_c$ s higher than 585°C, reaching up to 630°C (e.g. DENA.83, Fig. 5), which can be interpreted in terms of partially oxidized (titano)magnetite or (titano)maghemite. The reversibility of these curves indicates that this is thermally stable. Clear indication of the presence of hematite was rarely encountered in the  $KT$  curves.

#### 4.3.3 Hysteresis and IRM measurements

Magnetic hysteresis and IRM acquisition curves have been measured for a selection of samples spanning the range of material encountered in the studied structures (H in Table 1). Some typical curves are shown in Fig. 6. In most cases saturation is approached

by 300 mT and the hysteresis curves have a simple, narrow shape. IRM acquisition curves are square-shaped and also reach saturation at fields below 300 mT. This all indicates the dominance of low-coercivity minerals (e.g. (titano)magnetite and/or maghemite). The ascending and descending branches of the hysteresis curves are indistinguishable and linear at fields >300 mT, indicating a dominant control by paramagnetic (most probably clay) minerals. Hysteresis parameters (coercivity,  $H_c$ , saturation magnetization,  $M_s$ ) have been calculated after correcting for the paramagnetic contribution. Saturation remanence ( $M_{rs}$ ) and the coercivity of remanence ( $H_{cr}$ ) have been calculated from the IRM acquisition curves. The influence of high-coercivity minerals, most probably hematite, is seen in a minority of samples. IRM acquisition curves do not reach saturation by 500 mT, the maximum applied field. Here, wasp-waisted hysteresis loops attest to the presence of mixtures of low- and high-coercivity minerals.

The magnetization and coercivity ratios have been plotted on a Day plot (Day *et al.* 1977) (Fig. 6). Most of the data fall within the 'pseudo-single domain' region of the plot, with a trend parallel to the single and multidomain magnetite mixing curves as given by Dunlop (2002). The results are interpreted in terms of mixtures of single domain and multidomain material. Whilst the former probably dominates the stable NRM properties, multidomain material is present in significant amounts. Similar results have been seen in other archaeomagnetic studies (e.g. Schnepf *et al.* 2004). The various material types are not differentiated, indicating uniform magnetic mineralogy across most of the sampled structures. A group of samples exhibit  $H_{cr}/H_c$  ratios >5. They correspond to samples with wasp-waisted loops and unsaturated IRM curves, caused by the presence of a mixture of high- and low-coercivity minerals. In such mixtures the high-coercivity material has a greater effect on  $H_{cr}$  and gives rise to the elevated  $H_{cr}/H_c$  values. This data cannot be used to infer domain states.

#### 4.3.4 TRM anisotropy

Chauvin *et al.* (2000) demonstrated that the correction of NRM and TRM measurements using the TRM anisotropy tensor is needed

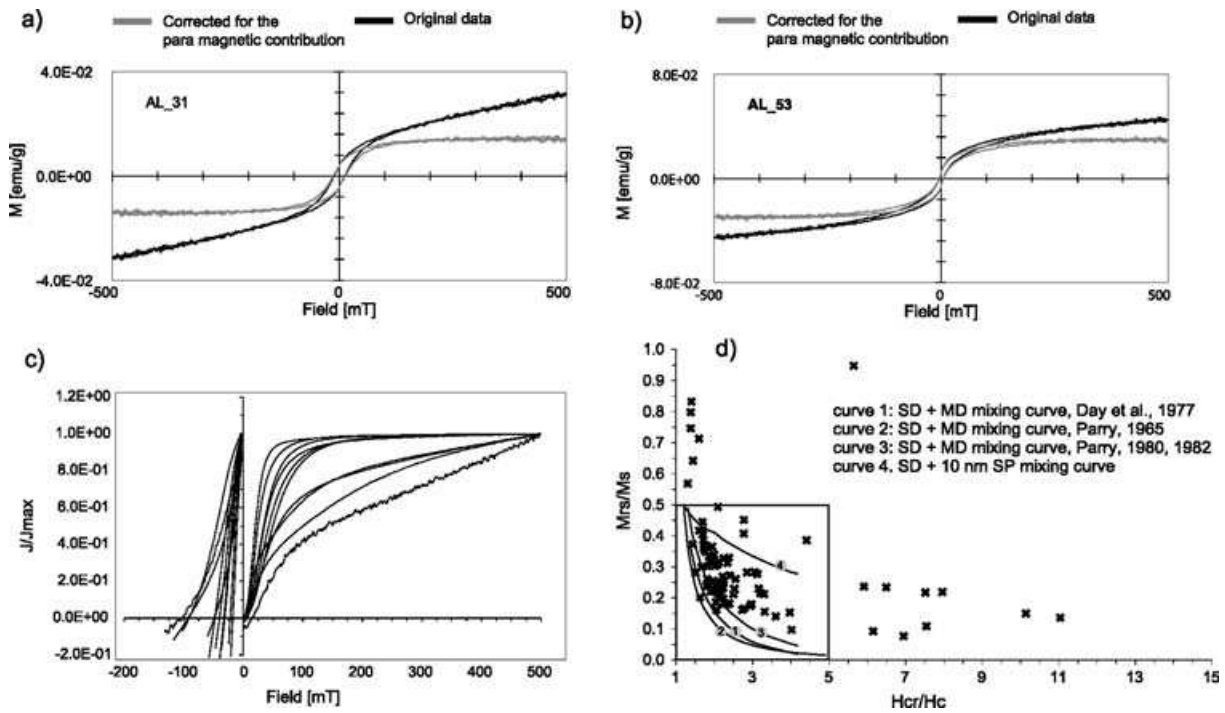


**Figure 6.** (a)–(c) Representative hysteresis and isothermal remanent magnetization and backfield curves. The curves after correcting for the paramagnetic contribution are shown in grey. (d) Day plot of hysteresis ratios. The mixing models of Dunlop (2002) are shown.

in order to obtain accurate archaeomagnetic results from tiles or bricks studied by Thellier-style experiments. For this reason, TRM anisotropy has been studied for 21 of the 25 structures studied in Rennes (AT in Table 1). The results show that the degree of anisotropy (the ratio of maximum and minimum axes of the TRM anisotropy tensor,  $k_1/k_3$ ) is usually <15 per cent, and that the principal axes do not show any systematic directional properties. Correcting for TRM anisotropy leads to little or no change in the mean ChRM directions, due to the random distribution of the TRM anisotropy axes and the low degree of anisotropy. For all the studied structures there is no clear dominance of magnetic lineation or foliation, except for the kiln MURO where foliation dominates. However, the characteristic directions of this kiln remains similar before and after TRM anisotropy correction. Typical behaviour is illustrated in Fig. 7 (PATH, structure 57 in Table 1). The directions of the principal TRM anisotropy axes are randomly distributed (Fig. 7a) and the Flinn diagram (magnetic lineation  $L$  ( $k_1/k_3$ ), versus the magnetic foliation  $F$  ( $k_2/k_3$ )) shows no clear dominance of either  $L$  or  $F$  (Fig. 7b). For the structures studied here correction for TRM

anisotropy is not important. This can be explained by the fact that the majority of sampled material is composed of baked clay or a mixture of bricks and baked clay. Nonetheless, all of the results labelled AT in Table 1 have been corrected for TRM anisotropy.

### 5 NEW ARCHAEOMAGNETIC DIRECTIONS

Site-mean directions have in all cases been calculated following a hierarchical structure (i.e. specimen → independently oriented sample → site). When more than one specimen was available from an independently oriented sample (drilled core or block sample), a mean sample direction was calculated using all of the specimens (for sites TH and AF in Table 1) or the most reliable demagnetization experiment was retained (for sites TH in Table 1). This choice was made on the basis of the larger fraction of NRM lost during Thellier experiments.

As can be seen in Table 1, the number of individual directions retained for mean computation ( $N$ ) is often lower than the number

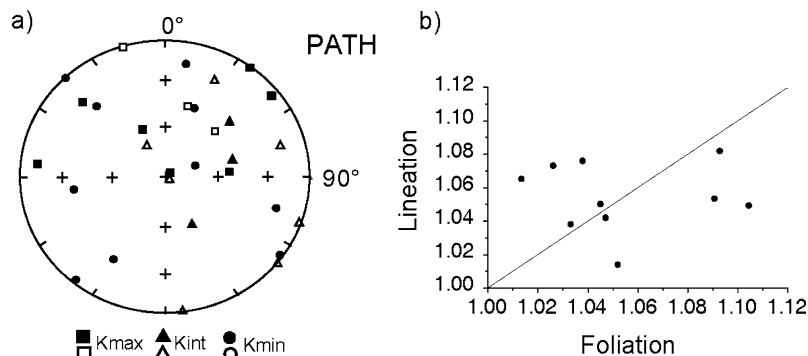


**Figure 7.** (a) Stereoplot of TRM anisotropy directions and (b) Flinn diagram for structure PATH (structure 57 in Table 1).

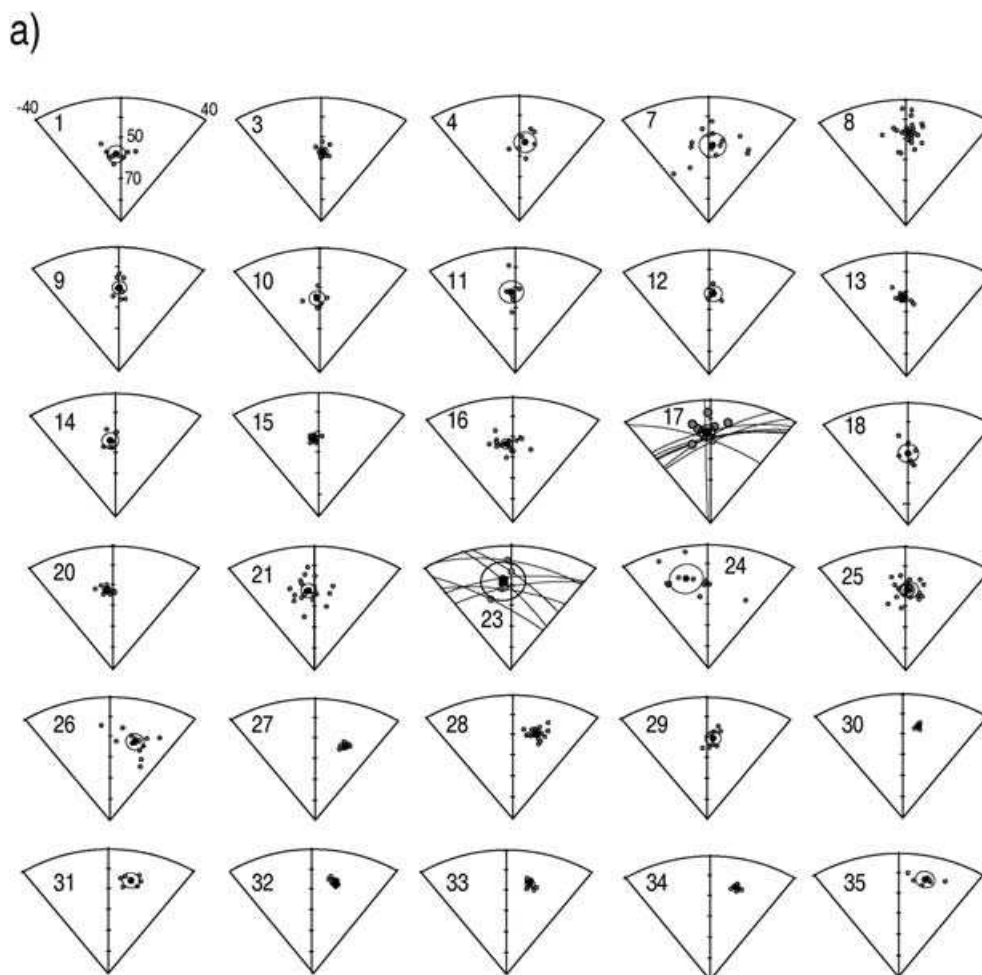


**Figure 8.** (a) and (b) Stereoplots of ChRM directions at the sample level (grey symbols), together with the mean direction and  $\alpha_{95}$  (in black) for each of the new structures studied. Where remagnetization circles have been used to determine site directions, the great circles used in the calculation are shown.

of independently oriented samples collected ( $N'$ ). This is related mostly to drilled samples that have been discarded because of potential orientation errors, and in some cases to samples that were lost due to the difficulty in preparing specimens from poorly consolidated blocks.

The mean directions for each structure were calculated using Fisher (1953) statistics. Generally, more than seven mean (independently oriented) sample directions have been used in the calculation of the mean site direction. For the five structures that exhibited two stable directions, the mean of the common (i.e. archaeomagnetic) directions was calculated using the remagnetization circle method or by a combination of this technique and principal component analysis (McFadden & McElhinny 1988).

For every site or structure the sample directions have been tested to see if they show a Fisherian distribution. Deviations from a Fisher distribution are assumed to arise through undetected orientation errors or to incomplete resolution of the ChRM (due to partial heating). In those structures showing non-Fisherian distributions, the sample direction showing the largest angular distance from the mean was discarded and the distribution recalculated, the process being repeated until Fisherian conditions were met. The results from 12 structures (and a total of only 4 per cent of the samples measured) have been modified in this way. In only four structures have more than two samples been discarded, corresponding to those that have suffered partial heating. Therefore all site mean directions have been

calculated from Fisher distributed directions. The resulting directional distributions are shown in Fig. 8.

The 58 new directions are shown in Table 1, along with the previously published data described earlier. Each site direction has been transferred to Madrid ( $40.4^\circ\text{N}$ ,  $3.7^\circ\text{W}$ ) via the virtual geomagnetic pole (VGP). The age distribution of the data set spans approximately 2000 yr. The oldest studied structure is dated at between 150 and 50 BC and the youngest at 1959 AD, and there is a gap between the 6th and 10th centuries where no data are available. For Roman, Medieval and Modern times several archaeomagnetic directions per century are available.

All of the data are represented in Fig. 9. Structure 45, which has no available dating error information, has been plotted with an arbitrary error of  $\pm 200$  yr. Structures coming from the same site and with the same age estimation give very similar results, for example the four pottery kilns from Patio Cardenal (structures 9–12, Table 1) or the seven kilns from Murcia c/Puxmarina (structures 31–37, Table 1). There is a very good agreement for the declination values. However, inclination sometimes shows a higher between-site dispersion, for example between 1500 and 1600 AD.

Six structures have been studied for this period (54–59, Table 1), four of which give very similar results, whereas two (PATJ, 56, and PATB, 58, Table 1) exhibit higher inclinations which are more consistent with later periods. These structures have relatively large uncertainties associated with their archaeological age estimates (see

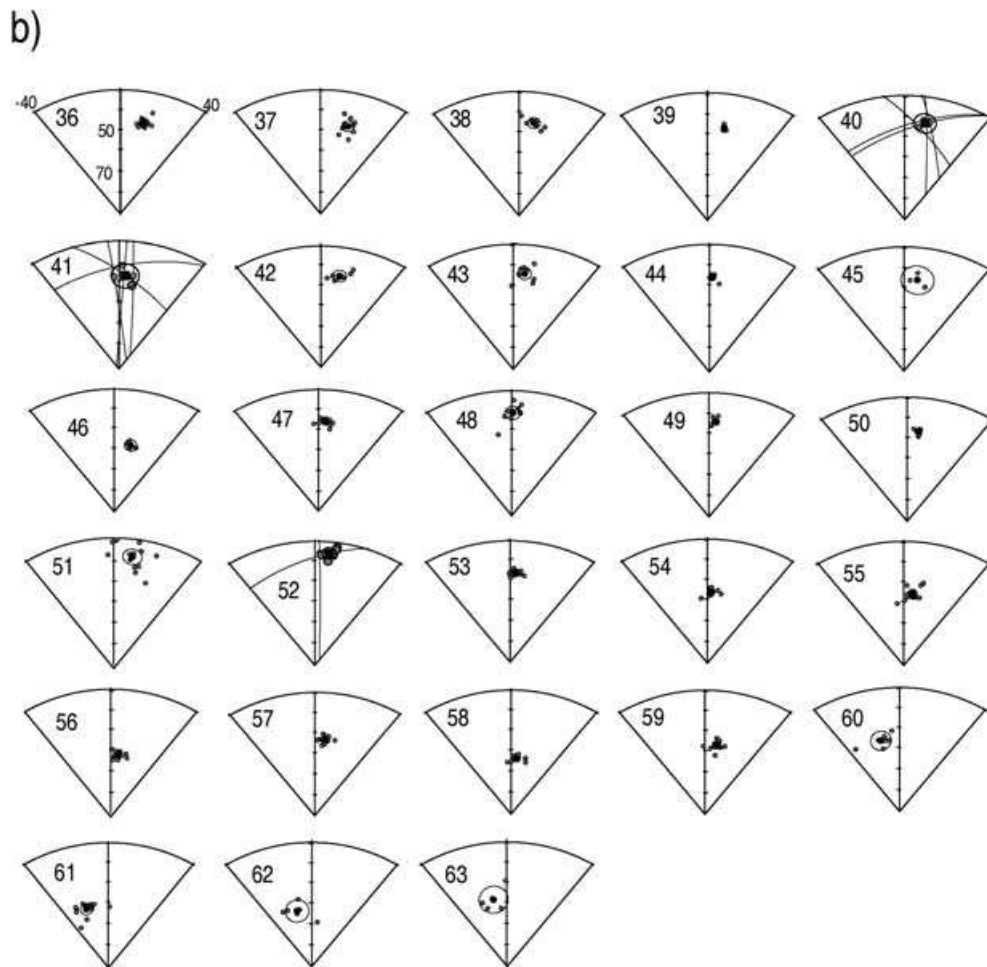


Figure 8. (Continued.)

Appendix), and considering their true age as being nearer the 17th century (rather than in the middle of the proposed interval) might explain the high inclinations. Alternatively, the structures may have suffered post-abandonment local movements, although archaeological observations and the large size of the structures do not support this idea. Irrespective of the explanation of the inclination variation, it should be noted that the dispersion observed in the inclination data is similar to that seen in other archaeological data (e.g. Schnepf *et al.* 2004).

The data from GUA1 (structure 46 in Table 1) is offset from the other data from the 14th century AD. This discrepancy may be explained by the lack of archaeological information (see Appendix). The age of the kiln is placed at  $1300 \pm 25$  AD, but no information is available to propose a reliable TPQ or TAQ for the structure. The mean value from PG1 (structure 24 in Table 1) is offset from the mean value of PG2 (number 25 in Table 1), but taking into account the large errors of PG1 the data are in agreement. These two structures, from the same archaeological site, are considered coeval on the basis of the archaeological information (see Appendix). Direct observations of the geomagnetic field for the Iberian Peninsula since 1858 obtained at the magnetic observatories of Lisboa, Coimbra and San Fernando (see Gaibar-Puertas 1953, for the data obtained at San Fernando) are also plotted on Fig. 9. They agree well with the modern archaeomagnetic directions for structures 62 and 63, taking into account the errors in the archaeomagnetic data.

In order to compare the Spanish data with the French SV curve (Gallet *et al.* 2002), the Spanish data have been recalculated for the latitude of Paris and plotted together with the French data (Fig. 10). The anomalous inclination obtained for GUA1 is also in disagreement with the inclination values given by the French SV curve, suggesting that the assigned archaeological age of 1300 AD may be questionable. For the rest of the data a good agreement with the French SV is observed.

## 6 CONCLUSIONS

A compilation of 63 archaeomagnetic directions has been presented, comprising five previous results and 58 new results. The types of archaeological structures range from ceramic and brick making kilns and furnaces, ovens, burnt walls and burnt floors. All have yielded stable and well-defined site-mean directions that have been calculated following a hierarchical structure. The use of remagnetization circle analysis for partially heated structures has improved the definition of the archaeomagnetic direction associated with relatively low-temperature heating. Rock magnetic studies indicate that the magnetic signal is dominated by magnetite or Ti-poor titanomagnetite. Thermally stable (titano)maghemite or partially oxidized magnetite has also been recognized, and in a few cases the influence of hematite has been observed.

The compiled data span approximately 2000 yr, from 100 BC to 1959 AD. Throughout most of the record several directions per



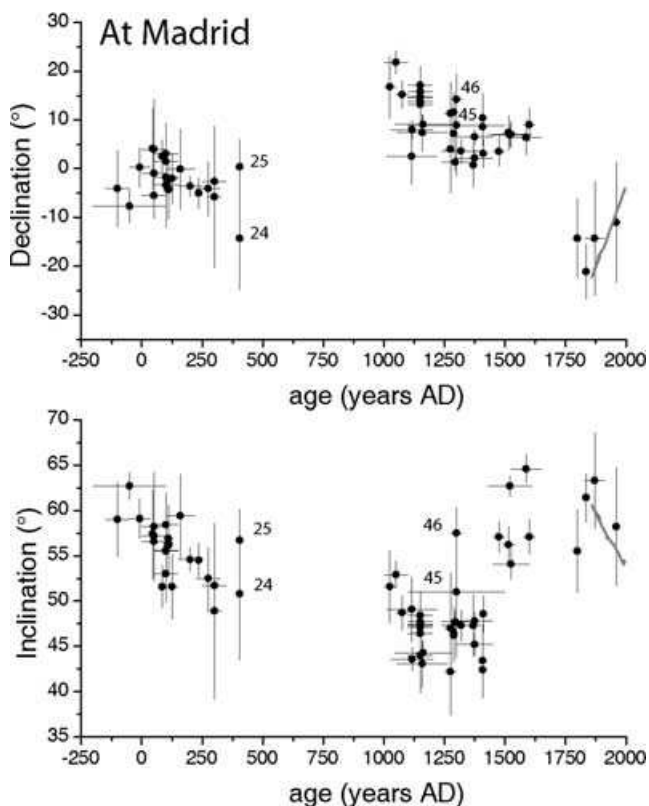


**Figure 9.** Declination and inclination versus age (reduced to Madrid). One site (structure 45 in Table 1) where no age error is available is plotted with an error of 200 yr, although there are no archaeological constraints. Direct observations from the Iberian Peninsula are plotted in grey.

century are available, although there is a gap in the data between the 6th and 10th century. The data are in broad agreement with the French SV curve of Gallet *et al.* (2002). There is a need to extend the data, and to improve the precision of the periods covered. However, the results represent the first step in the construction of a SV curve for the Iberian Peninsula. This will provide an additional tool in the dating of archaeological remains in the region, and the data can be used to better constrain the behaviour of the Earth's magnetic field in Western Europe during the last few millennia.

## ACKNOWLEDGMENTS

MG-P and GC acknowledge fellowships from the AARCH Network (Archaeomagnetic Applications for the Rescue of Cultural Heritage), Contract EU: HPRN-CT-2002-00219. The authors would like to thank two anonymous reviewers for their constructive comments, which improved the manuscript both in substance and style.

## REFERENCES

Batt, C.M., 1997. The British archaeomagnetic calibration curve: an objective treatment, *Archaeometry*, **39**, 153–168.  
 Casas, L.I., Shaw, J., Gich, M. & Share, J.A., 2005. High-quality microwave archeointensity determinations from an early 18th century AD English brick kiln, *Geophys. J. Int.*, **161**, 653–661.  
 Chauvin, A., Garcia, Y., Lanos, Ph. & Laubenheimer, F., 2000. Paleointensity of the geomagnetic field recovered on archaeomagnetic sites from France, *Phys. Earth planet. Inter.*, **120**, 111–136.

Day, R., Fuller, M.D. & Schmidt, V.A., 1977. Hysteresis properties of titanomagnetites: grain size and composition dependence, *Phys. Earth planet. Inter.*, **13**, 260–267.  
 Dunlop, J., 2002. Theory and application of the Day plot (Mrs/Ms versus Hcr/Hc). 1. Theoretical curves and tests using titanomagnetite data, *J. geophys. Res.*, **107**, doi:10.1029/2001JB000486.  
 Fisher, R.A., 1953. Dispersion on a sphere, *Proc. Roy. Soc. London A*, **217**, 295.  
 Gaibar-Puertas, C., 1953. Variación Secular del Campo Geomagnético, Observatorio del Ebro, Tarragona.  
 Gallet, Y., Genevey, A. & Le Goff, M., 2002. Three millennia of directional variations of the Earth's magnetic field in western Europe as revealed by archaeological artefacts, *Phys. Earth planet. Inter.*, **131**, 81–89.  
 Jasonov, P.G., Nurgaliev, D.K., Burov, D.V. & Heller, F., 1998. A modernized coercivity spectrometer, *Geologica Carpathica*, **49**(3), 224–225.  
 Kirschvink, J.L., 1980. The least-squares line and plane and the analysis of paleomagnetic data, *Geophys. J. R. astr. Soc.*, **62**, 699–718.  
 Korte, M., Genevey, A., Constable, C.G., Frank, U. & Schnepf, E., 2005. Continuous geomagnetic field models for the past 7 millennia: 1. A new global data compilation, *Geochem. Geophys. Geosyst.*, **6**, doi:10.1029/2004GC000800.  
 Kostadinova, M., Jordanova, N., Jordanova, D. & Kovacheva, M., 2004. Preliminary study on the effect of water glass impregnation on the rock-magnetic properties of baked clay, *Stud. Geophys. Geod.*, **48**, 637–646.  
 Kovacheva, M. & Toshkov, A., 1994. Geomagnetic field variations as determined from Bulgarian archeomagnetic data. Part I: the last 2000 years AD, *Sur. Geophys.*, **15**, 673–701.  
 Kovacheva, M., Parés, J.M., Jordanova, N. & Karloukovski, V., 1995. A new contribution to the archaeomagnetic study of a Roman pottery kiln from Calahorra (Spain), *Geophys. J. Int.*, **123**, 931–936.  
 Lanos, Ph., 2004. Bayesian inference of calibration curves: application to archaeomagnetism, in *Tools for Constructing Chronologies: Crossing Disciplinary Boundaries*, Vol. 177, pp. 43–82, eds Buck, C. & Millard, A., Springer-Verlag, London.  
 McFadden, P.L. & McElhinny, M.W., 1988. The combined analysis of remagnetization circles and direct observations in paleomagnetism, *Earth planet. Sci. Lett.*, **87**, 161–172.  
 Nachasova, I.E., Burakov, K.S. & Bernabeu, J., 2002. Geomagnetic field intensity variations in Spain, *Phys. Solid. Earth, Engl. Transl.*, **38**, 371–376.  
 Oyamburu, I., Villalain, J.J., Osete, M.L., Zarzalejos, M. & Blasco, C., 1996. Estudio paleomagnético del yacimiento de Villa del Pañuelo (Villamanta, Madrid), *Geogaceta*, **20**, 1044–1046.  
 Parés, J.M., De Jonge, R., Pascual, J.O., Bermúdez, A., Tovar, C.J., Luezas, R.A. & Maestro, N., 1992. Archaeomagnetic evidence for the age of a Roman pottery kiln from Calahorra (Spain), *Geophys. J. Int.*, **112**, 533–537.  
 Schnepf, E. & Lanos, Ph., 2005. Archaeomagnetic secular variation in Germany during the past 2500 years, *Geophys. J. Int.*, **163**, 479–490.  
 Schnepf, E., Pucher, R., Reindeers, J., Hambach, U., Soffel, H. & Hedley, I., 2004. A German catalogue of archaeomagnetic data, *Geophys. J. Int.*, **157**, 64–78.  
 Tarling, D.H., 1983. *Palaeomagnetism: Principles and Applications in Geology, Geophysics and Archaeology*, Chapman and Hall, London.  
 Tauxe, L., 1998. *Paleomagnetic Principles and Practice*. Kluwer Academic Publishers, The Netherlands.  
 Thellier, E., 1981. Sur la direction du champ magnétique terrestre en France durant les deux derniers millénaires, *Phys. Earth planet. Inter.*, **24**, 89–132.  
 Thellier, E. & Thellier, O., 1959. Sur l'intensité du champ magnétique terrestre dans le passé historique et géologique, *Ann. Géophys.*, **15**, 285–376.  
 Veitch, R.J., Hedley, G. & Wagner, J.J., 1984. An investigation of the intensity of the geomagnetic field during Roman times using magnetically anisotropic bricks and tiles, *Arch. Sc. Genève*, **37**, 359–373.

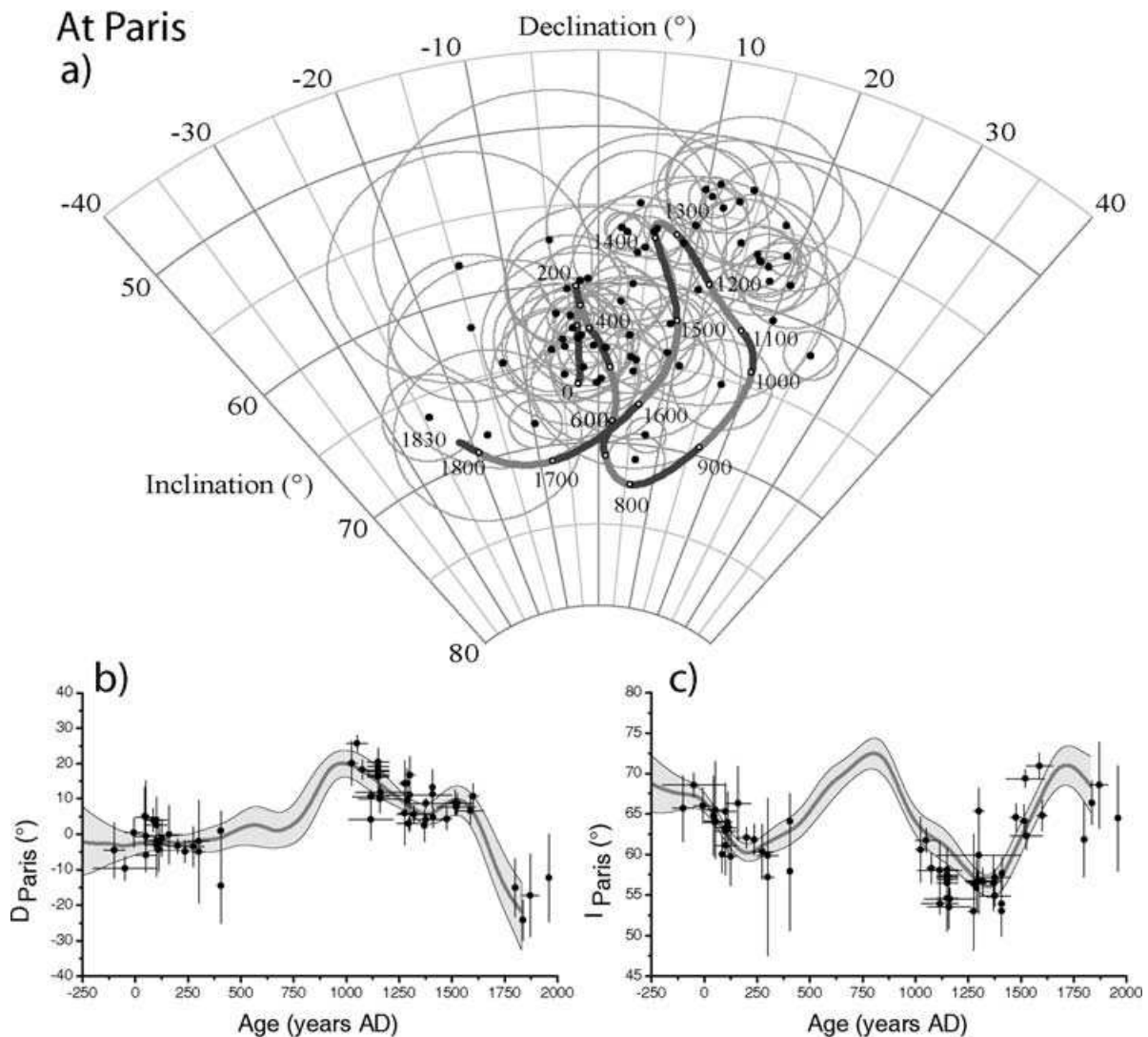


**Figure 10.** Comparison of the Spanish data with the French Secular Variation curve (Gallet *et al.* 2002) obtained by Bayesian modelling. The Spanish data have been reduced to Paris. (a) Stereographic plot, (b) declination and (c) inclination. The French SV curve is given in grey.

## APPENDIX: ARCHAEOLOGICAL AND CHRONOLOGICAL INFORMATION

This provides a summary of the archaeological sites and structures sampled, briefly describing where the samples were taken and the basis on which the structures have been dated. All block samples denoted as TH in Table 1 were taken by J. Thiriot, the remaining samples were taken by members of the UCM team (Spain). The *terminus post-quem* (TPQ) and *terminus ante-quem* (TAQ) are given where available. The TPQ (TAQ) indicates that the structures could be in use after (before) the given date.

The structures from each of the sites are set out below under the following heading:

*Site name (Province). Archaeologists in charge of the excavation. (structure number) laboratory structure name (archaeological structure name when different): age in years AD.*

### Plaza de Moros (Toledo). D. Urbina and C. Urquijo.

#### (1) PLM: $-100 \pm 50$ .

Plaza de Moros, Toledo, is considered a typical example of a fortified human settlement from the Second Iron Age (Urbina 2004).

It was destroyed following a fire which affected the whole of the site. Archaeomagnetic samples were taken from one of the burnt household walls.

The age is controlled by archaeological data and C14 dating. The general features are typical of Iron Age hillforts from central Spain. Archaeological constraints (ceramic fragments, metallic objects, decoration and painting style) place the site between the 4th and 2nd century BC (Cuadrado 1991; Fernández-Rodríguez 1987). No artefacts have been found above the stratigraphic layer associated with the fire and there is no evidence for later Roman occupation. On this basis the age of the fire has been placed at 150–50 BC (Urbina, private communication, 2005).

C14 dates have been obtained from two samples from a burnt wooden beam from one of the households, giving dates of 520–400 BC and 200 BC–20 AD. The different dates could represent different ages during the growth of the tree from which the beam was prepared. In this case the younger of the two will be closer to the age of the death of the tree—that is, when it was used in the construction of the house. The archaeologically constrained date of the fire is the preferred date (150–50 BC), pending resolution of the radiocarbon discrepancies.



**El Monastil (Alicante). A.M. Poveda-Navarro.****(3) MON:  $-7.5 \pm 42.5$ .**

Archaeological excavations in El Monastil, Alicante, revealed the remains of a pottery kiln. It has a square base, with part of the grill *in situ* and a semi-circular praefurnium (Poveda 1997, p. 482). Archaeomagnetic samples were taken from the baked floor and interior walls of the kiln.

The TPQ is based on ceramic fragments used in construction of the kiln, specifically mortar fragments and a fragment of amphora type Loma do Canho 67, providing an age of 1st century BC (Poveda 1997, p. 483). The TAQ is based on an amphora fragment found in the oven in-fill. The amphora, of the type Dr. 1—sigillata italica—Conspectus 22, is dated between 10 BC and 35 AD (Poveda 1997, p. 484). The age of abandonment has been placed between the second half of the 1st century BC and the TAQ (50 BC–35 AD).

**El Gallinero (Cádiz). I. Fernández-García. (4) GA:  $45 \pm 5$ .**

The area around Puerto Real, Cádiz, is a well-known zone of ceramic production (García-Vargas & Sibon-Olano 1995; Cepillo-Galvin & Blanes 2002). Excavations revealed a circular kiln, with a deteriorated grill supported by a central pillar with radial arcs. Archaeomagnetic samples were taken from the interior walls of the kiln.

Archaeological evidence, specifically the amphora types (Dr. 7, 8 and 10) produced in the area, indicates a period of activity around the second quarter of the 1st century AD (García-Vargas 1998, pp. 170–171), an age supported by later studies (Lagostena & Bernal 2004, p. 70). The age of abandonment of the site has been placed in the middle of the 1st century AD (40–50 AD).

**Costalita (Málaga). I. Navarro. (7) COS:  $50 \pm 50$ .**

The Roman site of Costalita was discovered in 2002 during construction works in Estepona, Málaga. Two excavations, 50 m apart, revealed the remains of a kiln used for manufacturing ceramics and construction materials ('*Pueblo Andaluz*'), together with the remains of a thermal bath (Suárez-Padilla *et al.* 2003; Suárez-Padilla *et al.* 2004). The kiln consists of a buried combustion chamber, with four adobe arcs supporting the grate. Each arc is in turn supported by two adobe pillars. The remains of the praefurnium have also been recognized. Archaeomagnetic samples were taken from the interior of the combustion chamber and from the praefurnium.

The age is controlled by archaeological data. Padilla *et al.* (2003) propose a chronology based on ceramic finds and on comparison with material from other Roman sites in the region. Ceramic fragments found during excavation can be ascribed to the 1st century AD. Some decorated fragments are similar to those found at the Venta del Carmen site (8, VC), which has been placed between the middle of the 1st century AD and the end of the 2nd century AD. A chronology centred in the mid-1st century AD (0–100 AD) is consistent with the materials recovered at the site and with the construction techniques of the kiln.

**Venta del Carmen (Cádiz). D. Bernal-Casasola.****(8) VC:  $85 \pm 5$ .**

The Venta del Carmen site is located close to Los Barrios, Cádiz. Two circular kilns, with grates supported by a central pillar, were excavated. In their last phase of use they were used as boilers (Bernal 1998; Bernal & Lorenzo 1998a), to which end a series of channels

and other structures were constructed. Archaeomagnetic samples were taken from the central pillar and the interior and exterior of the kiln wall.

The workshop has been placed between the Augustine and Flavian epochs (10 BC–90 AD), following evidence provided by imported goods (Italic and Gaulish sigillata, fine-walled ceramics, volute skylights and amphorae), along with the amphorae produced by the workshop itself (Bernal & Lorenzo 1998b). The age of abandonment of the site has been placed at 80–90 AD, just before sedimentary infilling of the kiln and nearby structures, which occurred at the end of the 1st century AD.

**Villares Andújar (Jaén). I. Fernández-García.****(9) VIA:  $100 \pm 50$ .**

Several kilns have been recovered from this well-known workshop near Andújar, in Jaén. The structure available for archaeomagnetic study was not excavated during the archaeological investigation of the site. It was exposed in a vertical cross-section in a road cutting. Archaeomagnetic samples were taken from the exposed kiln walls.

Archaeological considerations place the production period of the well-studied kilns as between the middle of the 1st and 2nd centuries AD (Fernández-García 2004, pp. 244–266). The sampled structure is considered as being coeval with the other kilns, between 50–150 AD, although this needs to be confirmed by further field investigations.

**Cartuja I-III (Granada). M. Orfila-Pons. (10–12)****CAR-HI, CAR-HII, CAR-HIII:  $100 \pm 50$ .**

Cartuja was an important Roman centre for manufacturing ceramic and building materials, located in the city of Granada. Excavations yielded 10 pottery kilns representing three phases of construction. Phase I dates from pre-1st century AD, phase II from the first half of the 1st century AD and phase III from between the second half of the 1st century and the first half of the 2nd century AD. Three kilns from phase III have been sampled for archaeomagnetic studies. Kiln HI, used in the manufacture of building material, is rectangular, with a grate supported by a double-arch structure and a well-preserved praefurnium. Archaeomagnetic samples have been taken from the interior kiln walls. Kiln HII is also rectangular, with a grate supported by four arches and two praefurniums representing different phases of construction. Archaeomagnetic samples have been taken from the interior walls of the firing chamber. Kiln HIII is rectangular, similar in structure to HI. It has a grate supported by four double arches and a large praefurnium with an adobe vault lined with bricks. Archaeomagnetic samples have been taken from the interior walls of the firing chamber and from the grate.

Archaeological data have been used to constrain their ages (Casado-Millán *et al.* 1999). Phases I–III have been distinguished on the basis of material recovered from the site (ceramics, building materials, coins, etc.) and on the ceramic styles produced at the site. The sampled kilns are from phase III and are considered to be coeval. An age of 50–150 AD has been ascribed to them.

**Patio Cardenal I-V (Sevilla). M.A. Tabales-Rodríguez.****(13–16) PAR1, PAR 3, PAR4, PAR5 (H-I, -III, -IV, -V):  $110 \pm 20$ .**

Archaeological excavations revealed one of the most important conserved workshops of Hispalis, the Roman city on which Seville

now stands (Tabales-Rodríguez 2003). In 'Patio del Cardenal', five circular kilns with circular central pillars supporting their grates were found, along with the remains of some large storerooms and some later rubbish dumps. Archaeomagnetic samples were taken from four of the kilns: PAR1—baked floor and interior wall of the kiln, PAR3—baked floor, interior wall of the kiln and central pillar, PAR4—interior wall of the kiln and central pillar, PAR5—baked floor and interior wall of the kiln.

Archaeological data have been used to date the kilns. The workshop mainly produced amphorae (types Dr. 20, Haltern 70, Dr. 28 and Beltran IIA, García-Vargas 2003). The proposed date of infilling/burial of the kilns is the second half of the 1st century AD, although some of the ovens could have been in use during the first decades of the 2nd century AD (Chic-García & García-Vargas 2003, p. 305). The kilns correspond to the final moments of the workshop, placed at 90–130 AD.

**Baelo Claudia (Cádiz). A. Álvarez-Rojas. (17) BC: 125 ± 25.**

'Baelo Claudia' is one of the best known Hispano-Roman sites, archaeological investigations since the beginning of the 20th century revealing the remains of a Roman city with a thermal complex which includes baths. The oven associated with heating the baths has been studied archaeomagnetically. Samples were taken from the praefurnium.

The site has been dated using archaeological information. Placed in the Low Imperial epoch by its excavators (Etienne & Mayet 1971), later studies improved on the original date, changing it to the middle of the 2nd century AD, maybe during the reign of Adriano (Sillieres 1995, pp. 161–162). The marks 'IMP.AVG' found on the bricks from the hipocaust are from a similar chronological period. The studied structure has been ascribed to the first half of the 2nd century AD (100–150 AD), based on archaeological considerations.

**Gallineras (Cádiz). A. Sáez-Espigares. (18) GAL: 160 ± 60.**

Gallineras, located in San Fernando, close to the city of Cádiz, is known as one of the main manufacturing centres of potteries and ceramics in southern Spain during Roman times. Excavations revealed a Roman villa, amphorae and seven kilns. Subsequent quarrying activity nearby lead to severe degradation of the site and only two of the seven kilns survived, one of which has been studied archaeomagnetically. Samples were taken from the praefurnium and interior wall of the kiln.

The area is rich in archaeological sites whose occupation date back from the 2nd to 8th century BC and it was an important production centre well into Roman times. The kilns at Gallineras are associated with the Roman villa, and have been dated using archaeological evidence. Ample pottery and amphora fragments have been recovered and engineering works in 1989 lead to the discovery of complete amphorae. Based on the style of the amphorae, and the recovered ceramics, Sáez-Romero *et al.* (2003) have proposed a principal age of kiln production ranging from the end of the 1st century BC to the 2nd century AD. However, some fragments from the early 3rd century AD have also been found and an age of 100–220 AD has been ascribed here in order to take this into account.

**Setla-Mirarrosa-Mirafior (Alicante). J.A. Gisbert-Santonja. (20) DENA (II): 235 ± 15.**

The kiln sampled (Setla-Mirarrosa-Mirafior) was discovered in a large handicrafts complex close to the coast (Gisbert-Santonja 1988; Gisbert-Santonja & Antoni 1991). Archaeomagnetic samples were taken from the interior walls of the kiln.

The age of this structure is archaeologically well constrained by findings of Amphorae (type Almadra IV), 3rd century AD pottery and coins. Note that the age control of Roman ceramics is well constrained for this period, allowing the definition of an age of 220–250 AD for the structure.

**Hyppolytus (Madrid). S. Rascón, J. Polo. (21) HIP (horno termas): 275 ± 50.**

Hyppolytus, near Madrid, is a complex of thermal baths associated with the Roman city of Complutum. One of the ovens associated with heating the baths has been studied archaeomagnetically. Samples were taken from the brick walls of the praefurnium.

The structure has been dated through archaeological investigations. Following extensive studies, the thermal complex and ovens have been dated as between the late 3rd century and the early part of the 4th century AD (225–325 AD), principally through ceramic finds and pavement types (García-Moreno & Rascon 1999).

**Valeria (Cuenca). A. Fuentes-Domínguez. (23) VAL (Casa de los Adobes): 300 ± 30.**

The ruins of the Roman city of Valeria, located close to Cuenca, have been under investigation since the early 1970s. The burnt wall of a building affected by a fire and subsequently abandoned has been studied archaeomagnetically. Samples were taken from the limestone blocks of the lower part of the burnt wall.

The TPQ/TAQ are defined by the lifespan of the city, known through archaeological considerations. It existed in the Low Imperial epoch, from the end of the 2nd century to the beginning of the 3rd century AD (TPQ), and was abandoned towards the end of the 4th century AD (TAQ). The date of the fire affecting the sampled building is placed at 270–330 AD by ceramics and coins found in association with the house (Fuentes 1988; Larrañaga 1995).

**Puente Grande I-II (Cádiz). D. Bernal-Casasola, L. Lorenzo. (24, 25) PG1 (Horno 1 del sector G), PG2 (Horno 2 del sector G): 405 ± 5.**

A large agricultural production centre, known as the Roman Villa of Puente Grande (Bernal & Lorenzo 2002, ed), was excavated in the Los Barrios district near Algeciras Bay. The site had two phases of occupation, and two circular kilns associated with the second occupation period have been studied archaeomagnetically. For structure PG1 samples were taken from the baked floor and walls of the combustion chamber. For PG2, samples were taken from the walls of the combustion chamber.

The site has been dated through archaeological information. No TPQ is defined, whilst the TAQ is well defined through coin finds. The first occupation phase has been placed in the 1st century AD, with subsequent abandonment during the Trajan epoch (Bernal & Lorenzo 2002a). The second phase, to which belong the excavated kilns, is placed between the 4th century and the early part of the 5th century AD (Bernal & Lorenzo 2002b). Ceramic fragments

(including African and southern Hispanic amphorae) and coins dated at 330–335 AD were found during excavation of the kilns (Lagostena & Bernal 2004, pp. 51–2), giving a period of production in the 4th century. The age of abandonment of the second occupation phase, hence the TAQ, is given by ceramic finds across the whole site, along with coins of age 348–395 AD, placing it in the first decade of the 5th century AD. There is no archaeological evidence of progressive abandonment and the studied kilns correspond with the abandonment phase of the villa, at 400–410 AD.

**Ramón Ortega I-II (Alicante). J.A. Gisbert-Santonja. (26) RO2 (U.E.125): 1025 ± 25, (28) RO1 (U.E.132): 1075 ± 25.**

Archaeological excavations in Denia ('Avenida Ramón Ortega'), revealed a complex of six Islamic, circular kilns which were found alongside a necropolis. Two of the kilns were chosen for archaeomagnetic studies. For both structures (RO1 and RO2), samples were taken from the walls of the firing chamber.

The structures have been dated through archaeological considerations (Gisbert-Santonja & Antoni 2000; Gisbert-Santonja 1997). The site is well dated through ceramic finds, kiln types and the general archaeological context (Gisbert-Santonja, private communication, 2004). The kilns have been placed in the 11th century AD, but are not considered coeval. RO2 is dated at 1000–1050 AD and RO1 at 1050–1100 AD.

**Murcia c/Sagasta (Murcia). J. Navarro-Palazón y F. Muñoz-López. (27) MURG (MUS 36.3): 1050 ± 50.**

Excavations in Murcia ('Calle Sagasta') revealed an Islamic pottery kiln. This kiln has been sampled for archaeomagnetic study, with samples taken from the interior walls of the kiln, which has been dated using archaeological data. Ceramic shards associated with the kiln have been dated as 11th century AD. The excavation of the levels overlying the kiln indicate urbanization of the area from the beginning of the 12th century. Therefore the kiln is considered to have been in use during the 11th century (Jiménez-Castillo, private communication, 2004).

**Cabrera d'Anoia (Barcelona). J.I. Padilla-Lapuente and J. Thirirot. (29) CDAP (99P): 1115 ± 105, (30) CDAU (99U): 1116 ± 87, (38) CDAJ (99J): 1159 ± 103, (39) CDAH (99H): 1162 ± 119.**

Cabrera Castle is located on a hill near the Anoia river valley, 50 km northwest of Barcelona. Around 40 Medieval, grey pottery kilns laying in a parallel series were found during excavations of the hillside substrata, four of which were sampled for archaeomagnetic study. Samples were taken from the interior walls of the kilns.

The grey pottery produced in this area is dated between the 9th and 15th century AD, and part of the production of the kilns is considered to have been for the castle occupants. The four studied kilns have been dated using the C14 method at the University Claude-Bernard of Lyon and the University of Barcelona (Padilla *et al.* 1998), giving ages that range from 1115 to 1162 AD.

**Murcia c/Puxmarina (Murcia). P. Jiménez-Castillo and J. Navarro-Palazón. (31) MURO (MUP99E), (32) MURN (MUP99D), (33) MURM (MUP99B) (34) MURL (MUP99A), (35) MURI (MUP131), (36) MURK (MUP185), (37) MURH (MUP22): 1150 ± 50.**

Excavations in Murcia ('Calle Puxmarina') revealed an abandoned, Islamic 'caliphal' house that had been converted into a glass-making workshop. Seven well-preserved Islamic kilns were found and all

were sampled for archaeomagnetic study. The samples were taken from the interior walls of the kilns.

The TAQ of these structures (1200 AD) is historically and archaeologically well constrained by the Christian conquest of the area in 1243 and by the construction of Islamic houses at the beginning of the 13th century. Ceramic finds and the general archaeological context indicate that the site was active during the 12th century but a well-defined TPQ is not available (Jiménez *et al.* 2000). The proposed abandonment date is between 1100 and 1200 AD. Note that MURL, MURM, MURN and MURO are four phases of the same kiln, MURL being the most recent.

**Magisterio I-II (Guadalajara). I. Ramírez-González. (40, 41) MAGI (MAG1), MAGII (MAG2): 1275 ± 25.**

Two kilns were revealed during excavations at El Magisterio, in Guadalajara. Both have been studied archaeomagnetically. Samples were taken from the kiln walls.

The structures have been dated through archaeological considerations. The kilns are considered coeval, and have been dated at 1250–1300 AD, principally through ceramic fragments found during excavations (Ramírez-González 2005a).

**Calatrava la Vieja (Ciudad Real). M. Retuerce and M.A. Hervás. (42, 43) CALA (CV218), CALB (CV250): 1287.5 ± 13, (53) CALC (CV252): 1410 ± 10.**

Calatrava la Vieja is an important site due that has been the object of numerous investigations (Retuerce & Hervás 2004). Occupied by Muslims from the 8th century AD, it was conquered in 1147 and became the first Templar possession in Castilla. After a brief Muslim occupation (1195–1212), it was reconquered and stayed in Christian hands until its abandonment at the beginning of the 15th century. Three kilns have been found at the site, all of which have been sampled for archaeomagnetic study. The samples were taken from the interior walls of the kilns.

The age of the kilns CALA and CALB is archaeologically and historically well constrained by ceramics and by the general context of the site. Ceramic finds correspond to the domain of the Calatrava Order, which held the castle after its reconquest in 1212, defining a TPQ for these two structures of 1212 AD. The age of abandonment is also constrained by ceramic typology and the general archaeological and historical context, and is placed at the end of the 13th century (1275–1300 AD).

The age of kiln CALC is controlled by archaeological data. It is placed between 1390 and 1420 AD on the basis of ceramic typology and the abandonment of the castle at the beginning of the 15th century (TAQ), which defines an age of abandonment of 1400–1420 AD.

**Valencia Velluters (Valencia). I. García-Villanueva. (44) VALN (VVE6009): 1294 ± 56, (47) VALI (VVE3734): 1319 ± 81, (49, 50) VALK (VVE4799), VALM (VVE5418): 1375 ± 75, (59) VALL (VVE5327): 1600 ± 25.**

Velluters, in Valencia, was located between the Islamic and Christian walls on the west side of Valencia. This area has been in continuous occupation since Medieval times. Several domestic, pottery and glass making kilns, related to different periods of occupation, have been discovered, five of which have been sampled for archaeomagnetic study. Samples were taken from the interior walls of the kilns.

The ages of the structures have been controlled primarily through archaeological considerations (García-Villanueva, private communication, 2004). Kilns VALI and VALN are probably Islamic kilns



which were in use until at least the Christian conquest of the area in 1238 AD, which defines their TPQ. The ancient access to VALI was buried beneath a surface from the second half of the 14th century. This places the TAQ at 1400 AD. VALN was covered by a ground level dated at the first half of the 14th century and was also affected by two holes, one of them filled with ceramics of the first half of the 14th century, allowing the definition of a TAQ of 1350 AD.

Kilns VALK and VALM were built on a ground level from the first half of the 14th century, and stratigraphically above the kilns another layer from the middle of the 15th century was found. This constrains the TPQ and TAQ of these structures to 1300 and 1450 AD, respectively. VALK, built on the top of the remains of VALM, is the younger of the two structures.

VALL was probably made in second half of the 15th century, in use during the 16th century and abandoned at the end of the 16th or the beginning of the 17th century. Ceramics from the late 15th – early 16th century were found within the kiln, establishing a TPQ of 1475–1525 AD. The TAQ, constrained by a covering layer containing well-dated ceramics from the end of the 16th century and the first quarter of the 17th century, is set at 1625 AD.

**Castillo de San Romualdo (Cádiz). A. Sáez-Espligares. (45) CSR: 1300 ± ?.**

Castillo de San Romualdo is unique in Spain, representing an Islamic kind of building known as a ‘*ribat*’ (a mixture of monastery and hillfort), supposed to have been built by Islamic masons who remained in Spain after the Christian reconquest. It is found in San Fernando, close to Cádiz. Archaeological excavations of the castle interior revealed seven different floor levels and a small adobe oven containing fired bricks. The oven has been studied archaeomagnetically. Samples were taken from the fired bricks found in the oven interior.

The age has been controlled using archaeological data. Little information is available about the exact origin of the castle, though due to its particular style of construction it is supposed to have been built in the late Middle Ages (before the end of the 14th century). The various floor levels, corresponding to different occupation phases have been dated using archaeological data. The first phase is interpreted as being from the low Middle Ages on the basis of ceramics, organic remains and bronze coins. The oven has been ascribed to a late Middle Age occupation level, placed in 1300 AD (Sáez-Espligares *et al.* 2001), with a lack of data preventing the definition of any error of this date.

**SUE-10 (Guadalajara). I. Ramírez-González. (46) GUA1: 1300 ± ?.**

Archaeological excavations at SUE 10—c/Ingeniero Mariño, in the city of Guadalajara, revealed the remains of a pottery kiln, two storage silos and domestic pottery fragments. Of the kiln, two pillars supporting the vault of the firing chamber and parts of the floor and walls of the combustion chamber were preserved *in situ*. Archaeomagnetic samples were taken from the two support pillars.

The kiln has been dated using archaeological data, principally through the construction technique used and the ceramics found in the silos. No strict TPQ/TAQ have been defined, and an age of 1300 ± 25 AD has been ascribed (Ramírez-González 2005b).

**Av. Blas de Infante (Cádiz). A. Torremocha. (48) BI (murallas Merinies, torres T3 y T4): 1369.**

The fortifications of Algeciras were destroyed during the 14th century Muslim reconquest of Algeciras. During the attack, the towers

and walls were first undermined, then the newly formed spaces were filled with wood which was then burnt, leading to the collapse of the towers and walls. Archaeomagnetic samples were taken from the fire-affected sandstone blocks from the base of the walls.

The date of the reconquest (hence the TPQ/TAQ of the burnt walls) is precisely controlled by historical documents. The chronicle of Enrique II places the year of the attack as 1369 AD. Muslim documents are more precise. The written communication of Ibn-al-Jat b states that the attack started on 1369 July 28, and that control of the city was acquired by July 31. A letter sent to Muhammad V al Jeque de la Meca in 1369 August supports these dates (Torremocha-Silva *et al.* 1999, 2000).

**Llano las Damas (Ceuta). D. Bernal-Casasola, J.M. Pérez-Rivera. (51) LLD: 1407.5 ± 7.5.**

Excavations in Ceuta, the Spanish enclave on the northern African coast, revealed a poorly conserved kiln. The kiln has been studied archaeomagnetically, with samples taken from the walls of the combustion chamber.

No firm TPQ is available. The kiln has been dated through historical and archaeological considerations, mainly ceramic finds. The proposed age of abandonment is between the second half of the 14th century AD and the Portuguese conquest of the city in 1415 AD (TAQ). Pending future investigations, the latter date is favoured, and an age of 1400–1415 AD has been ascribed.

**Huerta Rufino (Ceuta). J.M. Hita-Ruiz, F. Villada-Paredes. (52) HR: 1407.5 AD ± 7.5.**

Excavations in Ceuta, revealed an area of well-preserved Islamic houses. In one of the houses the remains of a kitchen with an oven and fireplace were identified. This oven/fireplace has been studied archaeomagnetically, with samples taken from the oven/fireplace hearth stones.

The structures have been dated through historical and archaeological considerations, although no details are available. Ceramic finds are placed between the second quarter of the 14th century and late 14th century. As with the previous site (51, LLD), the Portuguese conquest of the city in 1415 AD (TAQ) is favoured as the date of abandonment, and an age of 1400–1415 AD has been ascribed.

**Paterna c/Huertos (Valencia). M. Mesquida-García. (54) PATA (H21A): 1475 ± 25, (58) PATB (H21B): 1587.5 ± 62.5.**

**Paterna Testar del Moli (Valencia). M. Mesquida-García. (55) TMO: 1515 ± 25, (56) PATJ (H3B): 1520 ± 91, (57) PATH (41A): 1525 ± 75.**

The locality of Paterna is still known as a large pottery production centre. Two archaeological sites, at Calle de los Huertos and Testar del Moli have been studied (Mesquida-García 2002; Mesquida-García *et al.* 2001), with 5 kilns sampled for archaeomagnetic study. Samples were taken from the interior walls of the kilns.

PATA and PATB are two phases of the same kiln, PATB being the more recent. The phases have been dated using archaeological data. Ceramics from the 15th century have been found in association with the kiln. Archaeological constraints suggest abandonment of the first phase of the kiln took place between 1450–1500 AD, placing the TAQ at 1500 AD. The second phase of the kiln (with TPQ at 1450 AD) is said to have been in use for at least 75 yr (Mesquida-García, private communication, 2004), though a well-defined TAQ is not

available. In order to prevent any error in dating the last use of the structure, a large interval of 1525–1650 AD is proposed as the age of abandonment of PATB.

Archaeological data have been used to date TMO, although no details are available. The ascribed age is 1490–1540 AD.

PATH has been dated using archaeological data, ceramics from the end of the 14th century and the beginning of the 15th century giving a TPQ of 1375 AD. Archaeological constraints place the abandonment at 1450–1500 AD.

PATJ has been dated using the C14 method, giving an age of 1429–1611 AD.

#### **Monastery at Yuste (Cáceres). I. Ramírez-González. (60) YUS1: 1799 ± 15, (63) YUS2: 1959.**

The monastery at Yuste is an important historical site in Spain, being the site at which King Carlos V resided after his abdication in 1556. Archaeological investigations at the site revealed a completely preserved, large bread-making oven. Furthermore, a small oven was built by one of the monks in 1959, by the 'Casa del Obispo', next to the Monastery. This was an attempt to recreate traditional ceramic production methods. Both the historical and modern structures were sampled for archaeomagnetic study. For YUS1, samples were taken from the floor and interior walls of the cooking chamber. For YUS2, samples were taken from the walls of the firing chamber.

Both structures are well dated through archaeological, historical and anecdotal evidence. For YUS1, historical and archaeological considerations indicate the oven was in use during the life-span of the monastery. The TPQ, associated with the date of construction of the monastery, is not defined, although the site was occupied since at least the early part of the 15th century AD. The monastery was burnt to the ground during the Spanish War of Independence (1808–1814 AD), thus fixing the TAQ. The oven is considered to have been in use in the final decades up until the destruction of the monastery, and the age has been set between 1784 and 1814 AD (Ramírez-González 2000).

In 1949 AD the monastery was restored and in 1959 the modern kiln (YUS2) was built. It was abandoned in the same year because of a failure to produce acceptable ceramics.

#### **Huertas del Carmen (Guadalajara). I. Ramírez González. (61) GUA2: 1835 ± 10.**

Excavations related to construction works revealed a large brick-making furnace associated with the Convento del Carmen in Guadalajara. A large (>6 m<sup>3</sup>) combustion chamber and grate are preserved *in situ*. Archaeomagnetic samples were taken from the (vitrified) bricks of the interior walls of the combustion chamber.

The age of the furnace is controlled by archaeological and historical data. It is associated with the construction and maintenance of the Convent, which was built in 1632, which defines the TPQ. Documentary evidence of maintenance work associated with the sale of the Convent places the TAQ at 1845. The last use of the oven is considered to have been associated with this work. Ceramic finds support such a date (Ramírez-González 2005c).

#### **Palacio de Perales (Madrid). I. Ramírez González. (62) AL: 1870 ± 40.**

Archaeological excavations of the Palacio de Perales in Valdeolmos-Alalpardo, Madrid, revealed the remains of some perimeter walls,

baked clay paving stones and a buried cellar with well-conserved arcs. In one of the paved areas the outline of the remains of some kind of fire has been recognized. The paving stones affected are blackened and physically altered, and are readily distinguishable from unaffected areas. The burnt area has been sampled for archaeomagnetic study, samples being taken from an area of approximately 2 m<sup>2</sup>.

The TPQ is well constrained through historical documents, which state that the palace was built in 1730 AD for the Pinedo Family. After a century of occupation, the Palace suffered partial collapse and was eventually abandoned between 1830 and 1850 AD. Between the end of the 19th century AD and the beginning of the 20th century the palace was dismantled and the material recycled for use in new constructions, loosely defining the TAQ. The fire is associated with the period between the abandonment of the site and its dismantlement. It has been ascribed an age of 1830–1910 AD (Ramírez-González 2004, 2005d).

#### **References: Appendix**

#### **REFERENCES**

- Bernal, D., 1998. Excavaciones arqueológicas en el alfar romano de la Venta del Carmen (Los Barrios, Cádiz). Una aproximación a la producción de ánforas en la Bahía de Algeciras en época altoimperial, Madrid.
- Bernal, D. & Lorenzo, L., 1998a. Los hornos y las estructuras asociadas, en Excavaciones arqueológicas en el alfar romano de la Venta del Carmen (Los Barrios, Cádiz). Una aproximación a la producción de ánforas en la Bahía de Algeciras en época altoimperial (D. Bernal ed.), Madrid, pp. 81–120.
- Bernal, D. & Lorenzo, L., 1998b. Las cerámicas importadas y la cronología del complejo alfarero, en Excavaciones arqueológicas en el alfar romano de la Venta del Carmen (Los Barrios, Cádiz). Una aproximación a la producción de ánforas en la Bahía de Algeciras en época altoimperial (D. Bernal ed.), Madrid, pp. 63–80.
- Bernal, D. & Lorenzo, L., 2002. Excavaciones arqueológicas en la villa romana del Puente Grande (Los Altos del Ringo Rango, Los Barrios, Cádiz). Una ventana al conocimiento de la explotación económica de la Bahía de Algeciras entre el s. I y el V d.C., Huelva.
- Bernal, D. & Lorenzo, L., 2002a. Las cerámicas finas (TSI, TSG, TSH, TSA A) y otras cerámicas datantes (lucernas, paredes finas, africanas de cocina y engobe rojo pompeyano), Excavaciones arqueológicas en la villa romana del Puente Grande (Los Altos del Ringo Rango, Los Barrios, Cádiz). Una ventana al conocimiento de la explotación económica de la Bahía de Algeciras entre el s. I y el V d.C., Huelva, pp. 137–187.
- Bernal, D. & Lorenzo, L., 2002b. Las cerámicas africanas (TSA C y D) y la cronología de la fase bajoimperial, en Excavaciones arqueológicas en la villa romana del Puente Grande (Los Altos del Ringo Rango, Los Barrios, Cádiz). Una ventana al conocimiento de la explotación económica de la Bahía de Algeciras entre el s. I y el V d.C., Huelva, pp. 357–368.
- Casado-Millán, P.J., Burgos-Juárez, A., Orfila-Pons, M., Alcaraz-Hernández, E., Cassinello-Roldán, S., Cevidanes-León, S., Ruiz-Torres, S., 1999. Intervención arqueológica de urgencia en el alfar romano de Cartuja (Granada). Anuario Arqueológico de Andalucía 1994, vol. III. Actividades de Urgencia, Sevilla, pp. 129–139.
- Cepillo-Galvin, J.J. & Blanes, C., 2002. Informe- memoria de la intervención arqueológica de urgencia en las obras de limpieza y consolidación del horno romano de El Gallinero, Puerto Real (Cádiz), Anuario Arqueológico de Andalucía '99, III.1, Sevilla, pp. 73–77.
- Chic-García, G. & García-Vargas, E., 2003. Alfares y producciones cerámicas en la provincia de Sevilla. Balance y perspectivas, *Figlinae Baeticae*. Talleres alfareros y producciones cerámicas en la Bética romana (s. II a.C.—VII d.C.), British Archaeological Reports, International Series 1266, I, Oxford, pp. 279–348.
- Cuadrado, E., 1991. La cerámica ibero-céltica de barniz rojo, *Trabajos de Prehistoria*, 48, 341–356.

- Etienne, R. & Mayet, F., 1971. Briques de Belo: relations entre la Maurétanie Tingitane et la Bétique au Bas Empire, *Mélanges de la Casa de Velázquez* VII, Madrid, pp. 59–74.
- Fernández-García, M.I., 2004. Alfares y producciones cerámicas en la provincia de Jaén. Balance y perspectivas, *Figlinae Baeticae*. Talleres alfareros y producciones cerámicas en la Bética romana (s. II a.C.—VII d.C.), *British Archaeological Reports, International Series 1266*, I, Oxford, pp. 239–272.
- Fernández-Rodríguez, M., 1987. Cerámica de barniz rojo en la Meseta, *Archivo Español de Arqueología*, **60**, 3–20.
- Fuentes, A., 1988. La cronología del yacimiento hispanorromano de Valeria y su relación con otros análogos de la Meseta. *1º Congreso de Historia de Castilla - La Mancha*. T II, Ciudad Real, 211 ss.
- García-Vargas, E., 1998. La producción de ánforas en la Bahía de Cádiz en época romana (s. II a.C. – IV d.C.), Ed. Gráficas Sol, Écija.
- García-Moreno, L.A. & Rascon, S., 1999. Complutum y las ciudades hispanas en la Antigüedad Tardía. *Acta Antiqua Complutensia. N° 1*, pp. 7–23 (ISBN 84–8138–276–0)
- García-Vargas, E., 2003. Las producciones de la figlina. Ánforas, Arqueología y rehabilitación en el Parlamento de Andalucía. *Investigaciones arqueológicas en el Antiguo Hospital de las Cinco Llagas de Sevilla*, Sevilla, pp. 200–219.
- García-Vargas, E. & Sibon-Olano, F., 1995. Excavaciones de urgencia en el horno romano de El Gallinero (Puerto Real, Cádiz), *Anuario Arqueológico de Andalucía '92*, III, Sevilla, pp. 124–129.
- Gisbert-Santonja, 1997. 'La producción cerámica en Daniya-Dénia-en el siglo XI, *Cerámica Medieval e Pós-Medieval. Métodos e resultados para seu estudo*. Actas das 3as jornadas, 28 a 31 de Octubre.
- Gisbert-Santonja, J.A., 1988. 'L'Almadrava, Setla-Mirarosa-Miraflor, la Marina Alta, Alfar de ánforas romanas de finales del siglo I a principios del III d.C.', *Mémoires Arqueologiques de la Comunitat Valenciana, Educació y Ciencia de la Generalitat Valenciana*, Valencia, pp. 21–24.
- Gisbert-Santonja, J.A. & Antoni, J., 2000. Cerámica Califal de Dénia, *Universitat d'Alacant, Vicerectorat d'Extensió Universitària, Secretariat de Cultura*, Alacant.
- Gisbert-Santonja, J.A. & Antoni, J., 1991. El alfar romano de l'Almadrava (Setla-Mirarrosa-Miraflor) y la producción de ánforas e el territorio de Dianium, Aranegui Gascó, C., Saguntum y el Mar, pp. 114–116.
- Jiménez, P., Muñoz-López, F. & Thiriot, J., 2000. Les ateliers urbains de verriers de Murcia au XIIIe s. (C. Puxmarina et Pl. Belluga). *In: Pêtrequin, P., Fluzin, Ph., Thiriot, J., Benoit, P. dir.—Arts du feu et productions artisanales. XXèmes Rencontres internationales d'Antibes*, 1999. Editions APDCA, Antibes, 2000, p. 433–452.
- Lagostena, L. & Bernal, D., 2004. Alfares y producciones cerámicas en la provincia de Cádiz. Balance y perspectivas, *Figlinae Baeticae*. Talleres alfareros y producciones cerámicas en la Bética romana (s. II a.C.—VII d.C.), *British Archaeological Reports, International Series 1266*, I, Oxford, pp. 39–124.
- Larrañaga, J., 1995. Ruinas de Valeria. *N.A.H. II*, 153 ss.
- Mesquida-García, M., 2002. La cerámica de Paterna, *Reflejos del Mediterraneo*, Museo de Bellas Artes de Valencia.
- Mesquida-García, M., López-Peris, J.E., Prados, S. & Smolka R., 2001. Las Olleras de Paterna. *Tecnología y producción*, Volumen I. Siglos XII y XIII, *Ajuntament de Paterna*.
- Padilla, J.I., Thiriot, J., Evin, J. & Mestres, J., 1998. Datation par le radiocarbone des ateliers de potiers médiévaux de Cabrera d'Anoia en Catalogne. *Actes du colloque 'C14 Archéologie'*, pp. 419–423.
- Poveda, A., 1997. El horno romano (s. I a.C.) de El Monastil, XXIV Congreso Nacional de Arqueología, Elda, Alicante, pp. 481–493.
- Ramírez-González, I., 2000. Informe de la Intervención Arqueológica en el Monasterio de San Jerónimo de Yuste (Cuacos de Yuste, Cáceres), 2ª fase.
- Ramírez-González, I., 2004. Informe de Excavación arqueológica de la U.E.17, 18 y SAU n° 1 de Alalparto (Madrid).
- Ramírez-González, I., 2005a. Informe de la Excavación Arqueológica de la Escuela de Magisterio de Guadalajara.
- Ramírez-González, I., 2005b. Informe de la Excavación Arqueológica en el área de afección de la SUE 10 de Guadalajara.
- Ramírez-González, I., 2005c. Informe de Excavación Arqueológica en la Intervención Arqueológica en el área de afección de la SUE 20.5. de Guadalajara.
- Ramírez-González, I., 2005d. Informe de Excavación arqueológica de la U.E.17, 18 y SAU n° 1 de Alalparto (Madrid).
- Retuerce, M. & Hervás, M.A., 2004. Excavaciones arqueológicas en Calatrava la Vieja. Planteamientos y principales resultados. *Castilla La Mancha. 1996–2002. Patrimonio Histórico-Arqueología*. Castilla La Mancha, 18.
- Sáez-Espigares, A., Torremocha Silva, A. & Sáez Romero, A.M., 2001. Informes de las actividades arqueológicas desarrolladas en el castillo de San Romualdo. Campañas de 2000 y 2001. *Anuario Arqueológico de Andalucía/2001*, III, Sevilla, pp. 111–120.
- Sáez-Romero, A.M., Montero, R., Toboso, E.J. & Díaz, J.J., 2003. Control arqueológico en el yacimiento púnico-romano de Gallineras (San Fernando, Cádiz). *Anuario Arqueológico de Andalucía/2000*, III, Sevilla, pp. 166–173.
- Sillieres, P., 1995. Baelo Claudia. Une cité romaine de Bétique, Madrid.
- Suárez-Padilla, J., Tomassetti Guerra, J.M., Fernández-Rodríguez, L.E. & Navarro-Luengo, I., 2003. Un Horno Romano de época Altoimperial en El Saladillo. *Asociación Cilniana*, n 16.
- Suárez-Padilla, J., Tomassetti-Guerra, J.M., Bravo-Jiménez, S., Fernández-Rodríguez, L.E. & Navarro-Luengo, I., 2004. Un horno cerámico de época altoimperial en El Saladillo (Estepota, Málaga). D. Bernal/L. Lagostena, eds., *Figlinae Baeticae*. Talleres alfareros y producciones cerámicas en la bética romana (siglos II a.C.—VII d.C.), Cádiz.
- Tabales-Rodríguez, M.A., 2003. El complejo alfarero localizado bajo el Parlamento de Andalucía, Arqueología y rehabilitación en el Parlamento de Andalucía. *Investigaciones arqueológicas en el Antiguo Hospital de las Cinco Llagas de Sevilla*, Sevilla, pp. 139–162.
- Torremocha-Silva, A., Navarro Luengo, I. & Bautista Salado, J.B., 1999. Al-Binya, la ciudad palatina meriní de Algeciras. *Fundación Municipal de Cultura 'José Luis Cano'*, Algeciras.
- Torremocha-Silva, A., Navarro Luengo, I. & Bautista Salado, J.B., 2000. La Puerta de Gibraltar (Algeciras): un ejemplo de ingreso adelantado de época meriní en al-Andalus. *Caetaria*, 3, pp. 187–207.
- Urbina, D., 2004. Plaza de Moros (Villatobas, Toledo) y los recintos amurallados de la II Edad del Hierro en el Valle Medio Tajo. *Trabajos de Prehistoria*, **61**(2), pp. 155–166.